



Climatology of water
and energy cycles in
the Sahel

C. Velluet et al.

This discussion paper is/has been under review for the journal Hydrology and Earth System Sciences (HESS). Please refer to the corresponding final paper in HESS if available.

Building a field- and model-based climatology of local water and energy cycles in the cultivated Sahel – annual budgets and seasonality

C. Velluet¹, J. Demarty², B. Cappelaere², I. Braud³, H. B.-A. Issoufou⁴,
N. Boulain², D. Ramier^{2,5}, I. Mainassara^{6,7}, G. Charvet², M. Boucher^{2,8},
J.-P. Chazarin², M. Oï², H. Yahou^{4,7}, B. Maidaji^{4,6}, F. Arpin-Pont⁹, N. Benarrosh²,
A. Mahamane⁴, Y. Nazoumou⁷, G. Favreau², and J. Seghier²

¹Université Montpellier 2, UMR HSM (CNRS/IRD/UM1/UM2), Montpellier, France

²IRD, UMR HSM (CNRS/IRD/UM1/UM2), Montpellier, France

³IRSTEA, Unit HHLy, Lyon, France

⁴Université de Maradi, Biology Department, Maradi, Niger

⁵Cerema, DTer IDF, Trappes-en-Yvelines, France

⁶IRD, UMR HSM (CNRS/IRD/UM1/UM2), Niamey, Niger

⁷Université Abdou Moumouni, Geology Department, Niamey, Niger

⁸IRD, LTHE, Grenoble, France

⁹CNRS, UMR HSM (CNRS/IRD/UM1/UM2), Montpellier, France

Title Page

Abstract

Introduction

Conclusions

References

Tables

Figures

⏪

⏩

◀

▶

Back

Close

Full Screen / Esc

Printer-friendly Version

Interactive Discussion



Received: 9 March 2014 – Accepted: 7 April 2014 – Published: 13 May 2014

Correspondence to: B. Cappelaere (bernard.cappelaere@ird.fr)

Published by Copernicus Publications on behalf of the European Geosciences Union.

HESSD

11, 4753–4808, 2014

Climatology of water and energy cycles in the Sahel

C. Velluet et al.

[Title Page](#)

[Abstract](#)

[Introduction](#)

[Conclusions](#)

[References](#)

[Tables](#)

[Figures](#)

[|◀](#)

[▶|](#)

[◀](#)

[▶](#)

[Back](#)

[Close](#)

[Full Screen / Esc](#)

[Printer-friendly Version](#)

[Interactive Discussion](#)



Abstract

In the African Sahel, energy and water cycling at the land surface is pivotal for regional climate, water resources and land productivity, yet it is still extremely poorly documented. As a step towards a comprehensive climatological description of surface fluxes in this area, this study provides estimates of average annual budgets and seasonal cycles for two main land use types of the cultivated Sahelian belt, rainfed millet crop and fallow bush. These estimates build on the combination of a 7 year field dataset from two typical plots in southwestern Niger with detailed physically-based soil-plant-atmosphere modelling, yielding a continuous, comprehensive set of water and energy flux and storage variables over the 7 year period. In this study case in particular, blending field data with mechanistic modelling is considered as making best use of available data and knowledge for such purpose. It extends observations by reconstructing missing data and extrapolating to unobserved variables or periods. Furthermore, model constraining with observations compromises between extraction of observational information content and integration of process understanding, hence accounting for data imprecision and departure from physical laws. Climatological averages of all water and energy variables, with associated sampling uncertainty, are derived at annual to sub-seasonal scales from the 7 year series produced. Similarities and differences in the two ecosystems behaviors are highlighted. Mean annual evapotranspiration is found to represent $\sim 82\text{--}85\%$ of rainfall for both systems, but with different soil evaporation/plant transpiration partitioning and different seasonal distribution. The remainder consists entirely of runoff for the fallow, whereas drainage and runoff stand in a 40–60% proportion for the millet field. These results should provide a robust reference for the surface energy- and water-related studies needed in this region. The model developed in this context has the potential for reliable simulations outside the reported conditions, including changing climate and land cover.

HESSD

11, 4753–4808, 2014

Climatology of water and energy cycles in the Sahel

C. Velluet et al.

[Title Page](#)

[Abstract](#)

[Introduction](#)

[Conclusions](#)

[References](#)

[Tables](#)

[Figures](#)

[⏪](#)

[⏩](#)

[◀](#)

[▶](#)

[Back](#)

[Close](#)

[Full Screen / Esc](#)

[Printer-friendly Version](#)

[Interactive Discussion](#)



1 Introduction

In Africa, counterintuitive water cycle dynamics (Favreau et al., 2009) and prospects of increased water stress (Boko et al., 2007) or decreasing rain-fed agriculture yields (Schlenker and Lobell, 2010) challenge our ability to provide reliable projections of these key resources, especially in the densely populated, semiarid Sahel (rainfall $\sim 300\text{--}700\text{ mm yr}^{-1}$; Fig. 1a). Surface-atmosphere interactions are critical processes for the water cycle in this region. Strong evaporation recycles much of the rainfall to the atmosphere locally (Boulain et al., 2009b), and the surface feedback as vapor and radiative or turbulent energy plays a major role in atmosphere dynamics (Koster et al., 2004; Wolters et al., 2010; Taylor et al., 2011, 2012). Hence, meteorology, rainfall, and primary production all strongly depend on processes at the ground-atmosphere interface (GAI), as does recharge of surface ponds and of the underlying aquifer (Capelaere et al., 2009; Favreau et al., 2009; Massuel et al., 2011). Despite importance of these surface processes, quantitative knowledge on surface exchanges and ground-atmosphere interactions is still very limited in sub-Saharan Africa. Their distribution in space and time is all the more poorly documented. In the Sahelian domain of the West African monsoon, scarce field observations generally covered only short periods of time – typically a few days to a few weeks – at a few sites (e.g., Lloyd et al., 1997; Ezzahar et al., 2009; Timouk et al., 2009). Few studies covered a complete seasonal cycle (Wallace et al., 1991; Miller et al., 2009; Ramier et al., 2009). To our knowledge, none were based on a period of several years that is needed to capture the strong interannual variability of Sahelian rainfall. Current adverse public security conditions all over the Sahelian belt leave little hope that the complex type of instrumentation required (eddy covariance, scintillometry) could be significantly densified in the near future. In this context, remote sensing estimations are particularly promising for this region. However methods are still in development, and require context-specific field evaluation and calibration (e.g., Tanguy et al., 2012; Verhoef et al., 2012; Marshall et al., 2013). This is also true for model-derived estimates, as the ability of the current generation of land

HESSD

11, 4753–4808, 2014

Climatology of water and energy cycles in the Sahel

C. Velluet et al.

Title Page

Abstract

Introduction

Conclusions

References

Tables

Figures

⏪

⏩

◀

▶

Back

Close

Full Screen / Esc

Printer-friendly Version

Interactive Discussion



surface models (LSMs) to correctly reproduce dominant land processes in Africa is still largely in question (Boone et al., 2009a). Evaluating and improving the capabilities of general-purpose LSMs for this large continental region requires substantial reliable documentation of surface energy and water cycles at various time/space scales (Boone et al., 2009b).

When available, field estimates of surface fluxes are undoubtedly an invaluable asset. Nearly all components (radiative, conductive, turbulent) of the surface energy cycle are now more or less readily accessible to field estimation, even though this involves rather complex techniques and inhomogeneous representative scales. However these data are associated with uncertainty, particularly turbulent fluxes of sensible and latent heat. This uncertainty arises from a variety of sources such as instrumental error, departure of field conditions from underlying theory, or processing pitfalls (Foken et al., 2006; Aubinet et al., 2012). The general lack of energy balance closure that results from these estimation problems typically ranges 10–35 % of the available energy (Foken, 2008). Its assignment to the various possible sources is still a matter of debate (Aubinet et al., 2012). When estimation becomes unreliable, the corresponding data must be discarded. Added to recurrent interruption of sensitive equipment in hard field conditions (dust, temperature, wind), this generally leads to substantial gap rates in derived time series. For the surface water cycle, a number of components can hardly be field-measured precisely and continuously on a routine basis, e.g., overland runoff, vertical drainage and lateral subsurface flow, or partitioning of evapotranspiration into direct soil evaporation and canopy transpiration. For all these reasons – sparse data sets, unobserved components, uncertain data with conservation biases – it is not feasible to estimate complete and reliable water and energy balances at various time scales from field observations only, and some sort of modelling is thus necessary. Combining as many field observations as possible with physics-driven models that integrate available knowledge on the main local water and energy cycling processes, appears to be the most reliable way to make robust quantitative estimates of surface–atmosphere exchanges, in this region particularly.

Climatology of water and energy cycles in the Sahel

C. Velluet et al.

[Title Page](#)

[Abstract](#)

[Introduction](#)

[Conclusions](#)

[References](#)

[Tables](#)

[Figures](#)

[⏪](#)

[⏩](#)

[◀](#)

[▶](#)

[Back](#)

[Close](#)

[Full Screen / Esc](#)

[Printer-friendly Version](#)

[Interactive Discussion](#)



Climatology of water and energy cycles in the Sahel

C. Velluet et al.

Title Page

Abstract

Introduction

Conclusions

References

Tables

Figures

⏪

⏩

◀

▶

Back

Close

Full Screen / Esc

Printer-friendly Version

Interactive Discussion



The purpose of this paper is to present a detailed analysis of water and energy cycles for two plots that represent dominant land cover types in the cultivated Sahel, namely millet crop and fallow bush, over an unprecedented full 7 year period (Velluet, 2014). This is achieved by combining a unique field data set from the AMMA-CATCH¹ observing system in Niger covering that period (Boulain et al., 2009a; Cappelaere et al., 2009; Ramier et al., 2009) with the physically-based SiSPAT model of soil-vegetation-atmosphere transfers (Braud et al., 1995). This model has already been successfully tested over a short time period in this environment (Braud et al., 1997). The study area is located in the so-called central Sahel region, which is considered the most representative of the West African monsoon rainfall regime (Lebel and Ali, 2009). Available data include local rainfall and meteorology, vegetation phenology, all surface energy cycle components, soil moisture and temperature profiles. The SiSPAT model solves the 1-D-vertical equations for coupled diffusive transfers of water and heat in a heterogeneous soil, coupled with surface and plant exchanges with the atmosphere. It has been shown (Demarty et al., 2004; Shin et al., 2012) that even in the general heterogeneous, layered case, this type of soil water model can be reliably inverted for hydrodynamic properties from soil moisture observations when the profile is predominantly draining (no underlying moisture source), which is the case in nearly all of this region.

Previous GAI studies were carried out in the study area, either data-based (e.g., Miller et al., 2009; Ramier et al., 2009; Lohou et al., 2013) or model-based (e.g., Braud et al., 1997; Braud, 1998; Pellarin et al., 2009; Saux-Picart et al., 2009a, b). However they were limited to subseasonal periods or at most to one particular year. Models used were generally less detailed than in this study, in a more exploratory perspective. A major contribution of our multi-year analysis is that, for the first time to our knowledge, a climatological picture of water and energy surface fluxes at annual to subseasonal scales can be established for these main Sahelian land cover types. The continuous 7 year period allows capturing population averages for the variables investigated, while

¹African Monsoon Multidisciplinary Analyses – coupling tropical atmosphere and hydrological cycle; <http://www.amma-catch.org>.

minimizing the effect of possible decadal non-stationarities that appear to affect the monsoon and water cycle in this area (Lebel and Ali, 2009). Mean system behavior is highly informative as it carries the most robust features in the dynamics, enabling a powerful comparison of the two investigated systems. These results should contribute a substantial step to documenting the dynamics of surface fluxes in the Sahel. They provide robust reference information for evaluation and improvement of land surface models and remote sensing algorithms (Boone et al., 2009b). After a brief description of the sites, data, model, and methods used for the analysis (Sect. 2), results are presented successively for model calibration/skill and for the climatology of a synthetic average year from annual to subseasonal timescales (Sect. 3). Results significance and inferred information on processes are discussed in Sect. 4.

2 Materials and methods

2.1 Study area

The study area is located ~ 50 km east of Niamey, at 13.6° N– 2.6° E in the south-west of the Republic of Niger (Fig. 1). It consists of two plots of about 15 ha each, located ~ 0.5 km apart on the slope of the 2 km^2 Wankama catchment, in the AMMA-CATCH observatory (Cappelaere et al., 2009; Lebel et al., 2009). The plots consist of a millet field – millet is the single most important staple crop in the whole Sahel belt – and of a fallow field which is an integral part of the traditional cropping system. These are now by far the two main land use types in southwestern Niger (Leblanc et al., 2008; Descroix et al., 2009), as in much of the cultivated Sahel (van Vliet et al., 2013). Climate of the area is tropical semiarid, with average rainfall of $\sim 0.5 \text{ m yr}^{-1}$ and mean temperature of $\sim 30^{\circ}\text{C}$. It is typical of the West African monsoon regime, with a long dry season of ~ 6 months (November–April) with practically no rain, and a wet season with 30–50 convective storms concentrated mostly from June through September. Figure 2 shows this strong meteorological seasonality at Wankama, especially for rainfall, humidity and

Title Page

Abstract

Introduction

Conclusions

References

Tables

Figures

◀

▶

◀

▶

Back

Close

Full Screen / Esc

Printer-friendly Version

Interactive Discussion



wind, and to a lesser extent temperature. Soils are sandy, weakly structured, poor in nutrients and prone to surface crusting, with an unsaturated depth of several tens of meters (Massuel et al., 2006). Pearl millet (*Pennisetum glaucum*) is grown using traditional techniques, relying on rainfall and animal manuring with no irrigation and very little or no chemical fertilization. Sparse shrubs of *Guiera senegalensis* are left to grow in the crop fields and cut yearly just before the growing season (April–May). Before sowing, weeds are removed by shallow tilling with a hand hoe. After the first 5–10 mm of rainfall, traditional non-photosensitive varieties of millet are sown in pockets with a ~ 1 m spacing. Depending on subsequent rain or drought, it may need to be re-sown several times before plants can actually develop. Millet is harvested in late September or October, after the end of the rain season. Shrubs are allowed to grow again from any remaining soil moisture in the late monsoon, until the end of the dry season. The fallow vegetation typically consists of a shrub layer dominated by *Guiera senegalensis* (< 10³ individuals per ha, ~ 2 m high) and of a grass layer made of annual C3 and C4 species in variable composition, interspersed with bare soil patches (Boulain et al., 2009a). Traditional crop-fallow cycles used to alternate 10–20 years of fallow with 3–5 years of cropping, but with the acute need for food production this ratio is now almost reversed.

2.2 Field data and study period

At the start of the 2005 monsoon, the two plots were equipped with identical data acquisition setup for continuous recording of (i) meteorology: rainfall, air pressure, temperature and humidity, wind speed and direction, 4-component radiation; (ii) high-frequency eddy covariance for sensible and latent heat flux estimation: 3-D wind, temperature, and vapor concentration; (iii) soil variables: shallow ground heat flux, 2.5 m-deep temperature and moisture profiles. Details of this setup are given in Table 1. The millet plot was turned to cultivation just before the instrumentation began in 2005, while the fallow field had not been cropped since the early 2000s. In both plots, land use remained unchanged throughout the 7 year study period (May 2005–April 2012). Soil texture and

Climatology of water and energy cycles in the Sahel

C. Velluet et al.

Title Page

Abstract

Introduction

Conclusions

References

Tables

Figures

◀

▶

◀

▶

Back

Close

Full Screen / Esc

Printer-friendly Version

Interactive Discussion



bulk density were analyzed from samples taken over several 2.5 m-deep profiles at different dates through the period to calibrate soil moisture sensors for volumetric water content. Consistent particle size distributions of $\sim 84\text{--}92\%$ sand and $\sim 5\text{--}13\%$ clay were found at all profiles. Porosity was estimated from bulk density, in the range $0.32\text{--}0.36\text{ m}^3\text{ m}^{-3}$.

For the practical and theoretical reasons mentioned above, the data series include gaps of variable lengths (10–35 % missing data). Meteorological variables, needed for model forcing, were gap-filled by substituting the closest available data from similar instruments deployed over the Wankama catchment (Cappelaere et al., 2009). Eddy covariance data were processed into half-hourly turbulent fluxes, using *EdiRe* software (R. Clement, U. of Edinburgh) and CarboEurope recommendations (Mauder and Foken, 2004), as described in Ramier et al. (2009). Energy balance closure obtained with the different measured and estimated flux components is typical of what is commonly obtained with this type of instrumentation (Ramier et al., 2009). Extracts from these eddy covariance data have been extensively analyzed in various – local, regional, methodological – studies (e.g., Boulain et al., 2009a; Merbold et al., 2009; Ramier et al., 2009; Tanguy et al., 2012; Verhoef et al., 2012; Lohou et al., 2013; Marshall et al., 2013; Sjöstrom et al., 2011, 2013).

A field survey of vegetation phenology was conducted at the two plots every 1 or 2 weeks from June through December of all seven years (Boulain et al., 2009a). Of particular interest for this study are the height and leaf area index (LAI), in each layer of the ecosystem. LAI was derived from hemispherical images taken as prescribed by the VALERI project (<http://www.avignon.inra.fr/valeri>) and processed with Can-Eye software (Weiss et al., 2004). Additional information on the vegetation dynamics is available from biomass measurements, as well as from automatic cameras and radiometers especially for periods outside the growing season (e.g., shrub development in the millet field after cropping). These various information sources were used to derive a continuous daily LAI series for each plot and season over the study period (Fig. 3).

HESSD

11, 4753–4808, 2014

Climatology of water and energy cycles in the Sahel

C. Velluet et al.

Title Page

Abstract

Introduction

Conclusions

References

Tables

Figures

⏪

⏩

◀

▶

Back

Close

Full Screen / Esc

Printer-friendly Version

Interactive Discussion



Over this 7 year period, rainfall shows interannual variability in amount and timing in line with that reported for the Wankama catchment over the longer 1992–2006 period (Ramier et al., 2009), suggesting that our study period is representative of the general conditions prevailing in this area. Specifically, annual rainfall (values in Fig. 3) ranges from 350 to 580 mm yr⁻¹, with a mean and standard deviation of 465 and 81 mm yr⁻¹ respectively. Three years have similar, moderately below-average annual rainfall (420–430 mm yr⁻¹), but differ in the number (38–50), intensity, and time distribution of rain events.

2.3 Model principles

The SiSPAT model (Simple Soil–Plant–Atmosphere Transfer model; Braud et al., 1995; Braud, 2000; Demarty et al., 2002) was chosen for its ability to simulate the coupled heat and water exchanges through the soil-plant-atmosphere continuum on physical bases. As a SVAT (Soil–Vegetation–Atmosphere Transfer) column model, it is forced at a reference level with observed meteorology (rainfall, wind speed, air temperature and humidity, atmospheric pressure, incoming short and long wave radiation). Two energy budgets, one for the vegetation canopy and one for the soil surface, are solved concurrently and continuously for surface–atmosphere exchanges through the diurnal cycle, with temperature and humidity at the soil surface, at the leaf surface, and at the canopy level of the atmosphere as state variables. Leaf area is prescribed as time-variable LAI, and also conditions a rainfall interception reservoir. Turbulent fluxes are expressed using a classical electrical analogy in this two-layer system, based on the computation of a bulk stomatal resistance and of three aerodynamic resistances. The bulk stomatal resistance, representing the plant physiological response to climatic and environmental conditions, is modeled in terms of incoming global radiation, vapor pressure deficit and leaf water potential (Jarvis, 1976). The three aerodynamic resistances are determined using Shuttleworth and Wallace’s (1985) wind profile parameterization inside and above the canopy. Radiation transfers in the short and long wave bands account

Title Page

Abstract

Introduction

Conclusions

References

Tables

Figures

◀

▶

◀

▶

Back

Close

Full Screen / Esc

Printer-friendly Version

Interactive Discussion



for the two layer formalism with shielding and multiple reflection effects (Taconet et al., 1986).

A major model strength is its mechanistic representation of soil thermal and hydraulic dynamics, by solving the coupled equations of heat and mass transfer explicitly, including vapor phase. This allows in particular to account for strong heterogeneity in the soil profile, e.g., the common presence of a surface crust in this environment, or of several soil horizons with contrasted thermal and hydraulic conduction and retention properties. Different parameterizations of hydraulic conductivity and retention curves are possible. Each horizon is discretized for numerical solution of the dynamic and continuity equations, with variable node density in relation to magnitude of state variable gradients (e.g., higher near the surface or horizon boundaries). Water is extracted by plants based on a prescribed, constant or dynamic root density profile, assuming no plant storage (Federer, 1979; Milly, 1982). The above- and below-surface model components are coupled through soil surface temperature and humidity, leaf water potential, as well as conservation of energy and mass at the soil and plant surfaces. A lower boundary condition needs to be assigned for each of the heat and mass transfer equations at the bottom of the simulated soil column. Various boundary condition types, including Dirichlet and Neuman types, are proposed (Braud, 2000). The model is forced with meteorological data at a sub-hourly timestep to represent the diurnal cycle, and the data are linearly interpolated at the computational timestep. The timestep is adjusted automatically according to soil water pressure and temperature gradients. This enables accurate representation of process dynamics, e.g., when sharp variations occur during rain events, as well as satisfaction of numerical convergence and stability criteria.

The SiSPAT model has been previously applied to Sahelian sites near the study area (Braud et al., 1997; Braud, 1998), for relatively short simulation periods, but with encouraging results as to the model's ability to reproduce the Sahelian GAI behavior. It has also been used successfully in a variety of other complex, physics-oriented

HESSD

11, 4753–4808, 2014

Climatology of water and energy cycles in the Sahel

C. Velluet et al.

[Title Page](#)

[Abstract](#)

[Introduction](#)

[Conclusions](#)

[References](#)

[Tables](#)

[Figures](#)

[⏪](#)

[⏩](#)

[◀](#)

[▶](#)

[Back](#)

[Close](#)

[Full Screen / Esc](#)

[Printer-friendly Version](#)

[Interactive Discussion](#)



applications, such as isotopic tracing (e.g., Rothfuss et al., 2012) or remote-sensing simulations (e.g., Demarty et al., 2005).

2.4 Methodology

The SiSPAT model is forced for the fallow and millet plots with their 7 year (1 May 2005–30 April 2012) time series of half-hourly meteorological variables and daily LAI. A 4 m-deep soil domain is considered, to minimize possible errors in surface energy and water fluxes arising from assumed bottom conditions. These conditions are gravitational water drainage, and constant temperature equal to the observed multiyear average at 2.5 m depth. To allow for vertical non-homogeneity, the soil column is divided into five horizons named H1 to H5, to depths of 0.01, 0.20, 0.70, 1.20 and 4.00 m, respectively. The thin H1 horizon makes it possible to differentiate a surface crust from the soil proper. Separation of the latter into H2–H5 is derived from soil density profiles observed in the two fields. The 5-layer soil column is discretized into a total of 194 computation nodes to ensure accurate state variable profiles. These are initialized with soil water content and temperature profiles observed on 1 May 2005, linearly interpolated over the computation domain.

SiSPAT involves a rather large set of input parameters defining soil, vegetation, and surface properties (Table 2). Regarding soil properties, based on previous experience with the model for these Sahelian ecosystems (Braud et al., 1997; Braud, 1998), the water retention and conductivity curves for each horizon are parameterized using the van Genuchten (1980) – with Burdine’s (1953) condition – and the Brooks and Corey (1964) models, respectively. This leads to six hydrodynamic parameters (θ_{sat} , θ_r , K_{sat} , β , h_g , n) for each soil horizon (Table 2). For most model parameters, estimated values or plausible ranges are derived directly either from field observations or from the literature (Table 2). Note that pedotransfer functions are found of little help for prior conditioning of soil hydrodynamic properties, as ranges obtained are considerably larger than what is to be expected from the other information sources on these parameters

HESSD

11, 4753–4808, 2014

Climatology of water and energy cycles in the Sahel

C. Velluet et al.

Title Page

Abstract

Introduction

Conclusions

References

Tables

Figures

◀

▶

◀

▶

Back

Close

Full Screen / Esc

Printer-friendly Version

Interactive Discussion



(Velluet, 2014). Four groups of parameters – denoted A to D in Table 2 – are distinguished, differing in the way they are assigned values in this model implementation.

For groups A and B, assignment is completely independent of model operation. Group A consists of soil parameters derived from field measurements only, either directly, for texture and residual water content θ_r in each soil horizon, or indirectly, for the horizons' saturated water content θ_{sat} and thermal capacity, as well as for dry and wet soil albedos. θ_r is assigned the lowest water content measured within the horizon (Table 2). For lack of observation in H1, the lowest of all measured values is used instead. θ_{sat} is taken uniformly equal to 90% of average porosity, as this parameter displays little heterogeneity or model sensitivity. One reason for low sensitivity is that soil moisture remains far from saturation in this dry sandy environment (except locally within surface crusts during strong rain events). Dry heat capacity is estimated from porosity. Soil albedos are derived from 2-way shortwave radiation measurements in periods with no foliage. Parameters in group B (vegetation and soil emissivity, maximum stomatal resistance, vapor deficit factor in plant stress function, critical leaf potential, infrared interception parameter) are assigned from the literature only (Table 2).

Group C consists of additional vegetation parameters (total plant resistance, minimum stomatal resistance, vegetation albedo, short wave interception parameter, and root density profile) that are also assigned from values in the literature, however unlike group B they are slightly adjusted in final stage of parameter assignment, once group D parameters are calibrated. This enables fine tuning for some specific stages of the seasonal cycle (e.g., late monsoon, early dry season), when these parameters are most important. Root profiles are considered invariant for the fallow but seasonally-dynamic for the millet system. Finally, group D consists of soil parameters that cannot be ascribed prior values with sufficient accuracy, with respect to model sensitivity to these values, and are thus calibrated within prior ranges (Table 2). These are four hydrodynamic parameters – K_{sat} , h_g , n , β – and the soil thermal conductivity scaling parameter, for each horizon. Only two contrasted hydrological years (1 May 2006–30 April 2008) are used for calibration, the five remaining years being devoted to validation. Calibration

Climatology of water and energy cycles in the Sahel

C. Velluet et al.

Title Page

Abstract Introduction

Conclusions References

Tables Figures

◀ ▶

◀ ▶

Back Close

Full Screen / Esc

Printer-friendly Version

Interactive Discussion



Climatology of water and energy cycles in the Sahel

C. Velluet et al.

[Title Page](#)[Abstract](#)[Introduction](#)[Conclusions](#)[References](#)[Tables](#)[Figures](#)[⏪](#)[⏩](#)[◀](#)[▶](#)[Back](#)[Close](#)[Full Screen / Esc](#)[Printer-friendly Version](#)[Interactive Discussion](#)

is performed using a heuristic, stratified approach derived from prior sensitivity investigation, previous experience with the model (Braud, 1998; Boulet et al., 1999; Demarty et al., 2004, 2005), results from similar experiments (e.g., Ridler et al., 2012), and understanding of the physics of the various processes involved. All observed variables that are sensitive to a subset of parameters being calibrated are used for this purpose, at half-hourly timestep, with the aim of achieving the best compromise between these variables given their observability (accuracy, representativity). Several regularization rules are applied: (i) parameter values should remain within prior ranges; (ii) spatial variations (with depth and plot) in soil parameters should remain consistent with variations/similarities in observed characteristics. Impacts on the main evaluation variables (all energy fluxes, soil moisture and temperature profiles) are analyzed one parameter at a time, within its range, with the purpose of narrowing the latter conservatively. This analysis is repeated for every parameter in subset, and iterated several times until convergence is deemed acceptable. Finally the aforementioned slight adjustments are made to group C vegetation parameters.

In the next section, calibrated parameter values are discussed and the calibrated model is evaluated against all seven years of observations, revealing high model capability. The 7 year simulation is then used to estimate climatological averages for the water and energy fluxes at the two plots, at annual to subseasonal (running-monthly with a view to daily) timescales. Despite the limited sample size, sampling-induced uncertainty on estimated means is quite small. Combined with the high model skill, this small statistical uncertainty suggests that robust climatological features can be inferred from the analysis.

3 Results

Water and energy conservation is written hereafter with the following notation (Eq. 1):

$$P = R + D + Ev + Tr + dS/dt$$

$$SWin = SWout + IRnet + Rn \quad \text{with: } Rn = G + H + LE \quad (1)$$

$$\text{and: } IRnet = LWout - LWin; \quad LE = \lambda \cdot ET; \quad ET = Ev + Tr$$

where: P is precipitation, R runoff, D drainage below soil column, Ev direct soil evaporation, Tr plant transpiration, ET evapotranspiration, dS/dt water storage variation in soil column, Rn net radiation, $SWin$ global radiation, $SWout$ reflected solar radiation, $IRnet$ net infrared radiation, $LWin$ and $LWout$ down- and up-welling infrared radiation, G ground heat flux, H sensible heat flux, LE latent heat flux, λ latent heat of vaporization (units used hereafter are mm per unit time for P , R , D , Ev , Tr , ET and dS/dt , $W m^{-2}$ for $SWin$, $SWout$, $LWin$, $LWout$, $IRnet$, Rn , G , H and LE , and $kJ m^{-3}$ for λ).

3.1 Model calibration/validation

Assigned and calibrated parameter values are listed in Table 2. Dry and wet soil albedo values for the two plots are in good agreement with qualitative field indicators such as soil color and surface roughness. Soil hydrodynamic and thermal parameters in the H2–H5 horizons are consistent with the sandy texture, and exhibit moderate heterogeneity with depth and between sites, especially for the H3–H5 horizons. Among the van Genuchten–Burdine retention parameters, and relative to prior ranges, h_g is the most variable between horizons (–0.2 to –0.6 m), gradually with depth. Saturated hydraulic conductivity K_{sat} displays little variability across these horizons with values of 5×10^{-5} – $7 \times 10^{-5} \text{ ms}^{-1}$, on the upper side of the prescribed range. Most contrasting are the H1 hydraulic parameters, in accordance with surface crusting observed at the two sites that reduces permeability very substantially. A factor of 1 : 700 is found on K_{sat} between the surface and the underlying horizons at the fallow site. This factor is

lower (1 : 200) at the millet site, presumably due to the cultivation effort by the farmer. Similarly, the β parameter is found higher for H1 at both sites, further reducing shallow soil hydraulic conductivity. The n water retention parameter and the thermal conductivity scaling parameter are also different for the H1 horizon. Finally, values obtained for

vegetation resistance parameters agree very well with new experimental results at the fallow (Issoufou et al., 2013) and millet (Issoufou, unpublished data) sites. Statistics of model skill at half-hourly resolution (root mean square error RMSE, bias, correlation r , and Nash–Sutcliffe’s efficiency NSE) are shown in Table 3 for the whole 7 year period as well as for the calibration period alone. For both ecosystems, scores are overall very good, relative to the uncertainty that must be expected from these observations, and to what can generally be achieved when modelling these variables. A good balance is reached between the different types of evaluation variables, i.e., surface energy fluxes, soil moisture and temperature profiles. Scores for the two periods are of the same order, suggesting that although calibration uses only two years, it is quite robust across variable climatic and environmental conditions, without overfitting to those two years’ specifics. For many criteria, performance over the whole period is even slightly better, due a lower weight of the wettest year (2006) which the model reproduces a little less efficiently.

Overall, model skill appears positively related with the field-estimation precision that can be expected for each variable. Upwelling short-wave radiation is always very well simulated, with RMSEs in the order of 10 W m^{-2} ($\text{NSE} \approx 0.99$) for any period and site. Scores for long-wave radiation are also quite good, albeit with slightly higher RMSEs (in the range $15\text{--}18 \text{ W m}^{-2}$, depending on site and period; $\text{NSE} \approx 0.93\text{--}0.95$). Consequently, RMSEs of net radiation (R_n) are small, slightly higher for the millet plot ($<19 \text{ W m}^{-2}$ vs. $<15 \text{ W m}^{-2}$ for the fallow; $\text{NSE} \geq 0.99$), while R_n shows slight positive bias for the fallow ($\sim +5 \text{ W m}^{-2}$). This positive bias for R_n associated with negative biases for G (at -5 cm), H and LE , illustrates the lack of energy balance closure in the observations, which unduly penalizes model evaluation scores like bias and RMSE. Nonetheless, all these components appear on the whole to follow the high-resolution

HESSD

11, 4753–4808, 2014

Climatology of water and energy cycles in the Sahel

C. Velluet et al.

Title Page

Abstract

Introduction

Conclusions

References

Tables

Figures

◀

▶

◀

▶

Back

Close

Full Screen / Esc

Printer-friendly Version

Interactive Discussion



Climatology of water and energy cycles in the Sahel

C. Velluet et al.

Title Page

Abstract

Introduction

Conclusions

References

Tables

Figures

⏪

⏩

◀

▶

Back

Close

Full Screen / Esc

Printer-friendly Version

Interactive Discussion

observations quite well, consistently for both sites and all periods, and better for soil heat flux ($RMSE \approx 14\text{--}18\text{ W m}^{-2}$, $NSE \approx 0.92\text{--}0.95$) than for turbulent fluxes H and LE ($RMSE \approx 26\text{--}29$ and $\approx 26\text{--}39\text{ W m}^{-2}$, respectively; $NSE \approx 0.87\text{--}0.91$ and $\approx 0.76\text{--}0.78$, respectively). H and, to an even greater extent, LE are obviously the most difficult fluxes to measure accurately. In addition, the half-hourly time step is very challenging for modeling as it lies within the scales of turbulence, conferring fluctuations to the fluxes that the model does not resolve. For these reasons, calibration should not outweigh these observations, even though the variables are key with respect to the objectives pursued. The above scores compare very favorably with similar, state-of-the-art model applications, particularly for this type of climatic and environmental conditions. Biases in these fluxes are low, all below $\sim 5\text{ W m}^{-2}$ for the whole period ($<6\%$ of observed standard deviations). At daily timescale (excluding gappy days), overall RMSEs across sites fall at or below 9 W m^{-2} , and biases at or below 3 W m^{-2} , for all energy flux components and all available observations.

Soil water storage in the different horizons, as estimated from corresponding point measurements (from 0 to 2.5 m), is also very well reproduced (Table 3). This is especially true for the upper horizons showing significant dynamics, i.e., H1–H3 for the fallow ($NSE \approx 0.74\text{--}0.92$) and H1–H5 for the millet field ($NSE \approx 0.72\text{--}0.94$). The lower horizons H4 and H5 of the fallow only show very limited dynamics, and can thus hardly be evaluated with this criterion. Although the model seems to infiltrate a little too much water in the fallow's H4 horizon (slight positive bias), this is not very significant. The high correlation coefficients, for all periods, sites and horizons, demonstrate the model's ability to capture the soil water dynamics, in response to the variability of external forcings at timescales from event to interannual. This is further illustrated by Fig. 5 for total storage down to 2.5 m, at both sites through the study period. These results, obtained under contrasted hydrologic conditions for two ecosystems responding quite differently, are highly satisfactory.

Scores for soil temperatures show that these are very well reproduced at the millet site ($NSE \approx 0.72\text{--}0.96$), all the better as depth is smaller, i.e., as the impact of the

Climatology of water and energy cycles in the Sahel

C. Velluet et al.

Title Page

Abstract

Introduction

Conclusions

References

Tables

Figures

◀

▶

◀

▶

Back

Close

Full Screen / Esc

Printer-friendly Version

Interactive Discussion



bottom boundary assumption is lower and model physics is the main driver. Note that if in absolute terms deviations are higher near the surface (RMSE of 1.3–1.9°C at 0.1 m against 0.6–0.9°C below), these have to be related to the much larger variability, making model skill actually turn out better. The same is true also for the fallow plot, albeit with overall lower performance (NSE of 0.48–0.80, RMSE of 2.5–2.8°C at 0.1 m and 0.9–2.2°C below). In fact, most of this lack of fit consists of negative bias, which reaches –1.9 to –2.6°C near the surface, and decreases with depth due to tighter constraint by the boundary condition. This is also true, but to a much smaller extent, for the millet plot (bias is –0.4 to –0.6°C near the surface). Hence the temperature dynamics is actually very well represented, even for the fallow, both in phase (as testified by correlation), and in amplitude, only with constant underestimation. Such bias was already noticed in similar conditions (model and ecosystems) by Braud (1998), who attributed it to the 2-layer radiation conceptualization, when a significant bare soil fraction of the fallow plot actually receives radiation directly with no canopy shielding.

Finally, the high correlation values obtained at half-hourly timescale for both the energy fluxes and the shallow soil temperatures suggest that, in addition to event, seasonal, and interannual dynamics, the phasing of diurnal cycles is also very well represented by the model.

3.2 Climatology of the energy and water cycling at the GAI

Simulated variables are now analyzed in their distribution at annual, semi-annual, seasonal, and subseasonal scales over the study period, with the aim of estimating an average year for each site from this 7 year sample. Since differences in forcing fluxes (rainfall, incoming short and long wave radiation) between the two sites are all very small, these specific variables are not duplicated in the following.

3.2.1 Annual and semi-annual scale

The two pie charts in Fig. 6a display the distribution of the interannual mean water balance into its component parts for the fallow and the millet systems, respectively. It can be seen that: (i) direct soil evaporation is the largest component for both systems, and for the fallow particularly (60 % of total rainfall against 52 % for the millet field); (ii) canopy transpiration is the second largest in both cases, albeit lower in the fallow (25 %) than in the millet field (31 %); (iii) these two evaporative components result in quite similar total evapotranspiration for the two systems, which largely dominates the water balance (85 % and 82 %, respectively); (iv) runoff ranks next in magnitude for both systems, but is substantially larger for the fallow (15 % against 10 % for the millet field), (v) drainage (< 7 %) and to a lesser extent interannual 0–4 m soil storage variation (< 2 %) are significant in the millet system only (none in the fallow). Canopy interception/evaporation is found non-significant in both systems.

Because, at this largest timescale, differences between the two systems are much less substantial for the energy balance, a similar decomposition, in this case of total global radiation, is presented only for the average of the two systems (Fig. 6b). It shows that net infrared radiation is the main component (40 % of global radiation), closely followed by reflected solar radiation (31 %). Sensible heat ranks next (17 %), followed by latent heat (12 %). Soil heat flux is negligible at this scale of integration. When compared to a globe-averaged continental energy budget (Trenberth et al., 2009), all components are found larger at the study site, including latent heat. Regarding radiative losses, reflected short wave is closer to net infrared loss than it is globally. As for turbulent losses, sensible heat is greater than latent heat, contrary to globe averages.

Figure 7 displays in more detail the climatological water and energy balances for both systems, at annual scale and for two 6 month periods corresponding to the monsoon (May–October) and dry (November–April) seasons, respectively. Elemental components are also grouped by type: liquid vs. atmospheric vapor fluxes for water (Fig. 7a), radiative vs. turbulent for energy (Fig. 7b). Standard estimation errors are shown with

HESSD

11, 4753–4808, 2014

Climatology of water and energy cycles in the Sahel

C. Velluet et al.

Title Page

Abstract

Introduction

Conclusions

References

Tables

Figures

◀

▶

◀

▶

Back

Close

Full Screen / Esc

Printer-friendly Version

Interactive Discussion



5 estimated mean annual components, as well as ranges of the sample annual values. It can be seen that sampling uncertainty on estimated means is very small for all energy variables (max. standard error of 2.8 W m^{-2} , for latent heat flux in the fallow) relative to energy input (248 W m^{-2}). Relative to the 465 mm yr^{-1} rainfall, standard estimation error is higher for mean water balance components: up to 14.3 mm yr^{-1} for evaporation from fallow and 21.2 mm yr^{-1} for corresponding total evapotranspiration.

10 Results suggest that annual-scale differences between ecosystems – even though small for the energy balance – are statistically significant for most elemental components. Exceptions are turbulent (latent or sensible) heat fluxes, and also aggregated liquid fluxes. Hence, when switching ecosystems, tradeoffs occur at annual scale between runoff and drainage ($\sim 28 \text{ mm yr}^{-1}$, with more runoff for the fallow and vice-versa), between direct soil evaporation and canopy transpiration ($\sim 33 \text{ mm yr}^{-1}$, with more transpiration from the millet field and v.-v.), or to a lesser extent between short and long wave radiation losses ($< 6 \text{ W m}^{-2}$, with more long wave for the millet field and v.-v.). Stronger yet is the tradeoff ($\sim 50 \text{ W m}^{-2}$) between radiative and turbulent fluxes when switching seasons (more radiation in dry season and v.-v.), more particularly between infrared and latent heat losses – short wave and sensible heat are much less impacted, with only 9.3 and 6.6 W m^{-2} variation, respectively. Finally, when 6 month seasons are considered separately, sensible heat as well as wet-season transpiration and reflected solar radiation are not significantly different between ecosystems. In contrast, dry-season transpiration is much larger for the millet system with $\sim 23\%$ of annual total, against $\sim 4\%$ for the fallow.

3.2.2 Detailed seasonal cycle

25 We are interested here in the general pattern of variation of daily variables over an average year, as can be derived from the 7 year sample. Figures 8a and 9a display the estimated interannual mean seasonal courses of water and energy budget components, respectively. A 30 d running averaging was applied, to filter out high-frequency components and obtain a more robust estimate of the low frequency-dominated population's

Title Page

Abstract

Introduction

Conclusions

References

Tables

Figures

⏪

⏩

◀

▶

Back

Close

Full Screen / Esc

Printer-friendly Version

Interactive Discussion



Climatology of water and energy cycles in the Sahel

C. Velluet et al.

[Title Page](#)

[Abstract](#)

[Introduction](#)

[Conclusions](#)

[References](#)

[Tables](#)

[Figures](#)

[⏪](#)

[⏩](#)

[◀](#)

[▶](#)

[Back](#)

[Close](#)

[Full Screen / Esc](#)

[Printer-friendly Version](#)

[Interactive Discussion](#)



mean seasonal cycle (the value of this filtering is further discussed in Sect. 4.1.3). The sampling-induced standard estimation error is shown as a confidence interval for each variable. It can be seen that the sample of years enables interannual mean cycles to be derived with low statistical uncertainty, especially for most energy variables. Water cycle variables show somewhat larger relative uncertainties, with the noticeable exception of millet transpiration for which statistical uncertainty is very small ($< 0.14 \text{ mm d}^{-1}$).

Water

The rainfall signal displays the slightly-skewed bell shape, with a slow rise and sharp tail, typical of Sahelian rainfall seasonality (Fig. 8a). It is even strikingly close to the 1990–2007 mean seasonal cycle obtained for a $5^\circ \times 5^\circ$ window centered on the study site (Lebel and Ali, 2009), including: start/end timing, amplitude ($\sim 5.7 \text{ mm d}^{-1}$) and timing of peak, as well as of the successive phases of monsoon development (plateau in June, secondary peak and break in late July) and recession (plateau at the August–September turn) which are characteristic of the Sahelian monsoon regime.

Overall, seasonal soil evaporation and runoff follow rather homothetic general courses relative to the rainfall bell, smoother for evaporation, with maxima at 2.8 and 2.4 mm d^{-1} for evaporation and 1.1 and 0.8 mm d^{-1} for runoff at the fallow and millet sites respectively (Fig. 8a). However, when considering the corresponding ratio to concomitant rainfall (Fig. 8b), a general V-shape is obtained for evaporation, from ~ 0.8 at the beginning and the end of the season, down to a low of 0.5 (fallow) or 0.4 (millet) at monsoon peak. The shape is essentially opposite for the runoff ratio, in the range 0 – 0.2 (lower for the millet field than the fallow), albeit with a double peak: an absolute high in the 2nd half of July (cf. secondary rainfall peak, above, and peak rain intensity in Fig. 2a) and a relative high in late September, separated by a relative low at monsoon peak.

As transpiration is strongly buffered by the whole soil/vegetation system, it displays a very smooth course (Fig. 8a), lagged relative to rainfall by about 1 month for the fallow and 1.5 month for the millet system, and peaking around 1.5 mm d^{-1} (slightly higher

for the millet system). The lag in millet-field transpiration is to be related to the late phenological development of this ecosystem (Fig. 3), due in part to shrub management in the mixed crop-shrub farming. It is worth noting however that transpiration in the millet field peaks not only well after soil water content (storage inversion in Fig. 8a), but also slightly after LAI, with a growing contribution of the deep root zone (Fig. 10a). This may be traced both to (i) the downward extension of root extraction capacity that continues in that period – with shrub regrowth – in a wet subsoil (Fig. 10b), and (ii), maybe more importantly, to the dynamics of the energy budget, with sustained global radiation but vanishing soil evaporation, allowing for higher density of transpiration flux per unit leaf area.

Drainage from the millet plot at 4 m depth starts the latest of all fluxes (around beginning of September), peaks in October with limited intensity (max.: 0.3 mm d^{-1}), and recedes slowly over the dry season. Until nearly the end of September, all “consumptive” fluxes (runoff, evaporation, transpiration, but not drainage which starts just before) are substantially lower at the millet site than at the fallow, implying much higher storage/lower destorage up to then. This results in much higher water content in the millet plot through the whole average year, as illustrated by Fig. 10b for the root zone.

Energy

Due in particular to intertropical latitude and concomitance of the astronomical summer with the cloudier monsoon season, global radiation shows only limited seasonality ($230\text{--}275 \text{ W m}^{-2}$ range in average year), with two lows at winter solstice and peak monsoon, an absolute high in March, and a relative high, end of September (Fig. 9a). Yet seasonality is strong for all consumptive – radiative or turbulent – components of the energy cycle, and is essentially driven directly or indirectly by the single-pulse monsoon and associated water cycle dynamics. Only ground heat flux exhibits a bimodal response, but with small amplitude ($\pm 4 \text{ W m}^{-2}$). Direct control by water occurs mostly through latent heat, whose dynamics shows among all energy components (i) the largest amplitude, peaking at ~ 110 and 90 W m^{-2} for the fallow and millet plots

Title Page

Abstract

Introduction

Conclusions

References

Tables

Figures

◀

▶

◀

▶

Back

Close

Full Screen / Esc

Printer-friendly Version

Interactive Discussion



Latent heat is higher in the fallow from June to September (up to $\sim +21 \text{ W m}^{-2}$) and lower from October through most of the dry season (up to $\sim -21.5 \text{ W m}^{-2}$). The net radiation pattern is similar (up to $\sim \pm 15 \text{ W m}^{-2}$), albeit starting earlier (mid-April to \sim mid-September) and ending earlier (mid-October to mid-January) for the first and second periods, respectively. There is no significant difference in climatological ground heat flux between the two systems at this timescale. The evaporative fraction (part of latent heat in total turbulent heat flux, Fig. 9b) reaches around 0.9 in August in the fallow, vs. less than 0.7 in the millet field.

4 Discussion

4.1 Results significance

4.1.1 Representativity of study sites and period

To our knowledge, this is the first attempt to put forward a climatological view of GAI energy and water fluxes in the Sahel environment. While only two sites are considered in this study, a fallow bush field and a millet field, these are quite representative of dominant ecosystems in the Sahelian agricultural context. This not only applies to southwestern Niger but also to a very significant part of the whole sub-Saharan Sahelian belt. Variations obviously exist within this huge domain, depending on geology, monsoon specifics, population and agricultural practices, however first regional site inter-comparisons (Merbold et al., 2009; Sjöström et al., 2011, 2013; Lohou et al., 2013) evidenced strong similarities over the Sahelian domain, in sharp contrast with the other eco-climatic domains of tropical Africa. Hence, it is believed that the new results obtained at these two sites can serve as a useful reference well beyond the study area.

Previous studies (e.g., Braud, 1998; Verhoef et al., 1999; Miller et al., 2009; Ramier et al., 2009; Saux-Picart et al., 2009a) provided specific experimental and/or modeling results for surface fluxes in such ecosystems over much shorter periods, i.e. at scales

HESSD

11, 4753–4808, 2014

Climatology of water and energy cycles in the Sahel

C. Velluet et al.

Title Page

Abstract

Introduction

Conclusions

References

Tables

Figures

◀

▶

◀

▶

Back

Close

Full Screen / Esc

Printer-friendly Version

Interactive Discussion



ranging from a single event to at most an annual cycle. For instance, Miller et al. (2009) made a detailed field analysis of the surface energy balance at subseasonal to seasonal scales, based on a one-year record at a Niamey fallow site, i.e. in very similar conditions to ours. However, in light of the 7 year series studied here, it appears that the quite dry observation year (375 mm) at their site produced substantial flux anomalies, e.g. comparable latent and sensible heat fluxes at the height of the rain season. Such results could be misleading if they were considered alone. Conversely, the season analyzed by Ramier et al. (2009) was unusually wet (580 mm). This underlines the need for multi-year series to derive major features of surface response to variable monsoonal forcing. The unprecedented length of our study period for this region is a step in that direction. Seven years is probably a lower limit for producing robust results. However this seems a reasonable length in light of the rather small statistical uncertainty on estimated variables. Comparison of rainfall statistics for the 7 year period (interannual mean and variability, seasonal distribution) with longer records for the catchment (Ramier et al., 2009) or for the area (Lebel and Ali, 2009), suggests that our study period is quite representative of current monsoon conditions in the central Sahel. Accounting for non-stationarities in climate or in the hydro-ecosystem (land cover, soil) or for land management variability (e.g., crop/fallow rotation, cultivation practices, animal grazing/manuring) is another challenge facing the long-term observing system in operation in the Wankama catchment (Cappelaere et al., 2009). Now that a seemingly robust model has been developed for these ecosystems, it will be interesting to investigate additional years as more meteorological and phenological forcing data become available.

4.1.2 Model vs. data

When this study began, one question was whether field data alone would or not allow meeting the objectives. It was answered negatively for a variety of reasons. First, not all variables of interest are actually monitored (e.g., evapotranspiration partitioning, runoff, drainage). The second reason is that this type of dataset typically contains substantial

Climatology of water and energy cycles in the Sahel

C. Velluet et al.

Title Page

Abstract

Introduction

Conclusions

References

Tables

Figures

⏪

⏩

◀

▶

Back

Close

Full Screen / Esc

Printer-friendly Version

Interactive Discussion



Climatology of water and energy cycles in the Sahel

C. Velluet et al.

Title Page

Abstract

Introduction

Conclusions

References

Tables

Figures

⏪

⏩

◀

▶

Back

Close

Full Screen / Esc

Printer-friendly Version

Interactive Discussion



gaps, of variable duration and occurrence, which expose to significant errors and uncertainty in aggregations and statistics inferred directly. In our case, one fourth to one third of turbulent fluxes observations are missing after data-filtering (depending on variable and site; 11 to 18 % for other energy fluxes). Gap-filling techniques do of course exist, but they boil down to very basic data modelling, with crude hypotheses, which themselves may induce considerable errors and biases. Another problem with working from raw data only, is the usual limitations of field observations as for accuracy and representativity. The difficulties of obtaining reliable field estimates of surface fluxes are well known, especially for turbulent fluxes and even more so for evapotranspiration/latent heat flux (Foken et al., 2006), also for ground heat flux. Failure to close the energy budget by $\sim 15\text{--}20\%$ is generally observed, but this can reach over 30 % (Foken, 2008), casting substantial uncertainty on estimated fluxes. Part of the problem comes from the differences in measurement scales of the various fluxes or variables, from a point or a few cm^2 of soil to several hectares (variable in size and location depending on wind and atmospheric conditions for turbulent fluxes), with associated spatial heterogeneities. All these observational shortcomings would strongly hamper reliable estimation, from field data alone, of the dynamics of consistent and representative energy and water budgets at a given plot. Conversely, associating physics-based modelling to this rich dataset allows to (i) make all available field information work together instead of separately (across variable types and over time), (ii) constrain them with physical principles as regularization rules, to find the best compromise and make the most sense of all these different types of information/knowledge, (iii) produce output variables at a consistent, plot scale, obeying known physics, and as compatible as possible with the whole dataset.

Attempting to match a long and diverse set of observations – all high-resolution surface energy fluxes, soil moisture/temperature profiles – with a rather complex model, could be seen as quite a challenge. Results show that this is feasible for the two ecosystems and variable forcing conditions (Sect. 3.1), with parameters assigned in part from prior knowledge from the field and the literature, and in part from split-sample

calibration/validation (2 and 5 years, respectively). This was performed with a heuristic parameter adjustment method, based on expertise of the model, the data, and field properties and processes. In the authors' judgement, the compromise achieved in integrating the various data and regularization constraints is about the best possible. Some parameter equivalence does exist, however because of the strong conditioning by the wide range of control variables and simulation conditions, including those for validation, this should not affect the simulated trajectories unduly. In this study, model application is restricted in time to the observation period, which avoids extrapolating to weakly conditioned situations. However the calibrated model is thought to have the potential for reliable simulations well outside the observed conditions. Regarding unobserved fluxes, the fact that they may often occur separately in time (runoff during rainstorms, evaporation in the early rain season, transpiration during dry spells and in the early dry season) makes calibration of their main controlling parameters, and hence their simulation, all the more reliable.

4.1.3 Timescales of seasonal cycle analysis

Strictly speaking, because of the 30 d filtering applied to the simulated time series, the mean seasonal cycles produced (Figs. 8, 9 and 10) pertain to moving monthly quantities. However, the very smooth variations to be expected for the population's mean cycles should imply low sensitivity of the latter to time resolution below one month. Hence it is believed that the estimated seasonal courses of Figs. 8–10 provide rather good climatological estimates for finer timescales as well, down to daily resolution. Only the peaks (highs & lows), for this finest resolution, would be expected to be slightly smoothed out (underestimated maxima, overestimated minima). To give an idea of the possible differences between the population's daily and running-monthly mean seasonal cycles, we can simulate their relationship by applying a 30 d filter to the estimated seasonal signals of Figs. 8a and 9a: this reduces the seasonal standard deviation of water cycle variables by only 2 % (for soil evaporation) to 5 % (for runoff), and by 1.5 % (net infrared or latent heat) to 3 % (sensible heat) for all energy variables

Climatology of water and energy cycles in the Sahel

C. Velluet et al.

Title Page

Abstract

Introduction

Conclusions

References

Tables

Figures

◀

▶

◀

▶

Back

Close

Full Screen / Esc

Printer-friendly Version

Interactive Discussion



Climatology of water and energy cycles in the Sahel

C. Velluet et al.

Title Page

Abstract

Introduction

Conclusions

References

Tables

Figures

◀

▶

◀

▶

Back

Close

Full Screen / Esc

Printer-friendly Version

Interactive Discussion



but global radiation and ground flux ($\sim 7\%$). Note that these figures are quite stable with respect to recursive filter application, suggesting a robust approach. To obtain more rigorous, direct/unbiased estimates for the daily resolution, a record of considerable length would be needed to filter out sampling-induced high-frequency noise and ensure acceptable standard estimation error. To reach everywhere the same order of statistical uncertainty as with the estimations presented here, the required length is evaluated to vary from ~ 15 – 20 years for soil water storage or drainage in the millet field, to several centuries for rainfall, runoff, ground heat flux, or reflected shortwave (with > 2 decades for plant transpiration, > 3 decades for net infrared radiation, and 6–10 decades for soil evaporation and all turbulent heat fluxes).

Finally, as only the systems' mean behavior is investigated here, variability around climatological means is not reflected. Thus, it should be kept in mind that, at any timescale (daily to annual), some of the features highlighted by this first-order analysis may not hold at all times, and that they can even turn out to be the opposite under certain circumstances.

4.2 Insights into some key GAI processes

4.2.1 Runoff/infiltration, soil storage and drainage

Runoff values for the two sites are compatible with results from previous field plot studies in the area (e.g., Peugeot et al., 1997; Estèves and Lapetite, 2003). They show high variability, with annual runoff spanning a range of $\sim 120\%$ of mean for both sites, and annual runoff coefficient ranging 5.6–18.8% for the fallow and 2.6–13.3% for the millet plot. High runoff from the fallow is due in particular to a low hydraulic conductivity and high retention in the thin surface horizon (H1), representing the soil crust observed in the field. Lower runoff from the millet field is largely due to the comparatively higher conductivity/lower retention of its H1 horizon. However a sharp contrast with the underlying sandy soil (H2–H5 horizons) is also found, confirming that some degree of

in this environment. They also temper the hypothesized benefit that plants could draw during a growing season from subsurface moisture accumulated during the previous rainy season: while this does happen in our simulations for the millet field vegetation in the months just after the rain season ($\sim 7\%$ of rainfall, on average; Figs. 7a, 8a and 10a) and possibly to a limited extent for moisture carried over from one monsoon season to the next in the 1.5–2.5 m depth range (Fig. 10b), no comparable benefit appears for the fallow in this study.

Partly due to this late wet season/early dry season shrub regrowth in the millet field, the general picture of higher evapotranspiration from a fallow ecosystem than from a millet field (Gash et al., 1997; Ramier et al., 2009) is also somewhat moderated by our results. In this study, this is true on average during most of the rainy season (Fig. 8) – despite generally lower soil moisture –, but not in the late September–January period, making annual totals turn out very similar (fallow slightly above). Also, when considering interannual variability, rankings may revert both annually and/or at some periods of the wet season, likely in relation with higher short-timescale variability in transpiration for the fallow. This larger variability can be traced both to the lower and more variable soil storage (Fig. 10b) that makes fallow vegetation more exposed to rainfall shortage, and to the higher LAI variability (Fig. 3) reflecting higher ecosystem sensitivity to environmental conditions (Boulain et al., 2009a) and exposure to external factors such as pasturing.

Finally, our results also suggest that these contrasts in wet season evapotranspiration between the two ecosystems, originate at least partly from differences in generation of direct soil evaporation, which is clearly enhanced in the fallow field. Hence, higher rain season evapotranspiration from the fallow may not – only – be related to plant physiological effects on transpiration, but maybe more importantly to the physics of direct soil-atmosphere exchanges within these two ecosystems (e.g., differences in convective “shield” effect, cf. Tuzet et al., 1997, or in shallow soil properties). Whether this conclusion can be generalized requires further analysis.

Climatology of water and energy cycles in the Sahel

C. Velluet et al.

[Title Page](#)[Abstract](#)[Introduction](#)[Conclusions](#)[References](#)[Tables](#)[Figures](#)[⏪](#)[⏩](#)[◀](#)[▶](#)[Back](#)[Close](#)[Full Screen / Esc](#)[Printer-friendly Version](#)[Interactive Discussion](#)

5 Conclusion

The purpose of this work is to build upon a unique, multi-year record of local water and energy observations for two typical plots in south-west Niger, in order to propose for the first time a climatology of these processes in the Sahel region. The methodology used relies on the development of a detailed, physically-based column model that is finely calibrated against this important dataset. It provides a time/depth-continuous series of all water and energy cycles variables involved, over a full 7 year period. This includes unobserved variables, most notably direct soil evaporation, plant transpiration, runoff, and drainage. The model, forced with observed meteorology and phenology, is calibrated against two years of data and evaluated against the full seven years, showing very good skill in reproducing the whole observation record. For instance, the model is able to reproduce faithfully the observation of larger evapotranspiration in the fallow than in the millet plot during most of the rain season despite lower soil moisture. The variety of monsoon conditions encountered and of evaluation variables used – covering the full surface energy balance (short and long wave radiation, turbulent fluxes, soil heat flux), and 2.5 m-deep soil moisture and temperature profiles – offers a comprehensive set of constraints that ensures a reliable model trajectory.

The time series produced for all water and energy variables are analyzed statistically at several timescales: annual and seasonal aggregates, seasonal cycle of running-monthly to daily values. A detailed documentation of climatological mean water and energy cycling, with sample-related uncertainty, is thus presented. From this analysis, new insights are derived on the interplay between processes, that corroborate, refine or question some ideas proposed so far in the literature. Uncertainty sources other than time sampling are not considered quantitatively in this study, as this requires elaborate assumptions to be made for all possible error sources, which is an upcoming step of this project.

With evapotranspiration/latent heat representing over 80 % of the mean annual water budget and nearly half the energy budget in the peak monsoon, the case for studying

HESSD

11, 4753–4808, 2014

Climatology of water and energy cycles in the Sahel

C. Velluet et al.

[Title Page](#)

[Abstract](#)

[Introduction](#)

[Conclusions](#)

[References](#)

[Tables](#)

[Figures](#)

[⏪](#)

[⏩](#)

[◀](#)

[▶](#)

[Back](#)

[Close](#)

[Full Screen / Esc](#)

[Printer-friendly Version](#)

[Interactive Discussion](#)



Climatology of water and energy cycles in the Sahel

C. Velluet et al.

[Title Page](#)[Abstract](#)[Introduction](#)[Conclusions](#)[References](#)[Tables](#)[Figures](#)[⏪](#)[⏩](#)[◀](#)[▶](#)[Back](#)[Close](#)[Full Screen / Esc](#)[Printer-friendly Version](#)[Interactive Discussion](#)

these two strongly-coupled cycles jointly, and for resolving this coupling explicitly, is thus strongly supported for the Sahel region. The atmospheric vapor flux is shown to be dominated by direct soil evaporation during most of the monsoon season in the average year. Plant transpiration becomes dominant only in the last part of the wet season (starting in second half of September) and continuing into the beginning of the dry season. Differences between the two land cover types are substantial for most components of the water budget, but less so for the energy budget. All climatological water fluxes are higher in the fallow until around end of September, and over the whole wet season for runoff and soil evaporation; conversely, soil storage, drainage and dry-season plant transpiration are always larger in the millet field. Like latent heat, net radiation is higher (lower net infrared) in the fallow until late September, and vice-versa until the next monsoon (~ end of April). Differences in sensible heat are shorter-lived, with more pronounced extrema (high in May, low in August) for the fallow.

These qualitative and quantitative results should prove useful as reference field information for various purposes, such as evaluating and improving land surface models or remote sensing algorithms for the Sahelian belt, as undertaken for example in the framework of the ongoing ALMIP-2 project² (Boone et al., 2009b). To our knowledge, the study presented here represents one of the most extensive analyses of local field-scale water/energy cycling performed for the Sahelian context to date, associating both a unique dataset in length and quality and a very detailed, finely calibrated model. This climatological analysis is currently being extended to subseasonal variability around mean behavior, with the aim of providing comprehensive statistical signatures of surfaces fluxes to serve as reference for land–atmosphere studies. Observations are continuing at the Wankama site to extend model evaluation information and to evaluate effects of land management practices on the water and energy balances.

Acknowledgements. The first author's Ph.D. was financed by a student research grant from SIBAGHE Doctoral School at University Montpellier 2 (<http://www.sibaghe.univ-montp2.fr>). This work was made possible by data from the AMMA-CATCH observing system (<http://www>.

²AMMA Land Model Intercomparison Project – Phase 2.

amma-catch.org) in Niger, which is supported by IRD, INSU and OREME and is a component of the RBV research catchments network (<http://rnbv.ipgp.fr>). The study also benefited from partial financial support by ANR (ESCAPE project) and CNES (TOSCA programme). Fruitful discussions with A. Boone, V. Guinot, P. Hiernaux, M. Ibrahim, L. Kergoat, and C. Leduc are gratefully acknowledged. The authors also wish to thank IRD's local representation in Niger (<http://www.niger.ird.fr>) as well as the Wankama villagers.

References

- Allen, R. G., Pereira, L. S., Raes, D., and Smith, M.: Crop Evapotranspiration: Guidelines for Computing Crop Requirements, F.A.O., Rome, 300 pp., 1998.
- Aubinet, M., Vesala, T., and Papale, D.: Eddy Covariance – a Practical Guide to Measurement and Data Analysis, Springer Atmospheric Sciences, Springer, Dordrecht, 438 pp., 2012.
- Boko, M., Niang, I., Nyong, A., Vogel, C., Githeko, A., Medany, M., Osman-Elasha, B., Tabo, R., and Yanda, P.: Africa, in: Climate Change 2007: Impacts, Adaptation and Vulnerability, Contribution of Working Group II to the Fourth Assessment Report of the Intergovernmental Panel on Climate Change, edited by: Parry, M. L., Canziani, O. F., Palutikof, J. P., van der Linden, P. J., and Hanson, C. E., Cambridge University Press, Cambridge UK, 433–467, 2007.
- Boone, A., Decharme, B., Guichard, F., de Rosnay, P., Balsamo, G., Beljaars, A., Chopin, F., Orgeval, T., Polcher, J., Delire, C., Ducharne, A., Gascoïn, S., Grippa, M., Jarlan, L., Kergoat, L., Mougin, E., Gusev, Y., Nasonova, O., Harris, P., Taylor, C., Norgaard, A., Sandholt, I., Ottlé, C., Pocard-Leclercq, I., Saux-Picart, S., and Xue, Y.: The AMMA Land Surface Model Intercomparison Project (ALMIP), *B. Am. Meteorol. Soc.*, 90, 1865–1880, doi:10.1175/2009bams2786.1, 2009a.
- Boone, A., Getirana, A., Demarty, J., Cappelaere, B., Galle, S., Grippa, M., Lebel, T., Mougin, E., Peugeot, C., and Vischel, T.: The AMMA Land Surface Model Intercomparison Project phase 2 (ALMIP-2), *Gewex News*, 19, 9–10, 2009b.
- Boulain, N., Cappelaere, B., Ramier, D., Issoufou, H. B. A., Halilou, O., Seghieri, J., Guillemain, F., Oi, M., Gignoux, J., and Timouk, F.: Towards an understanding of coupled physical and biological processes in the cultivated Sahel – 2. vegetation and carbon dynamics, *J. Hydrol.*, 375, 190–203, doi:10.1016/j.jhydrol.2008.11.045, 2009a.

Climatology of water and energy cycles in the Sahel

C. Velluet et al.

Title Page

Abstract

Introduction

Conclusions

References

Tables

Figures

◀

▶

◀

▶

Back

Close

Full Screen / Esc

Printer-friendly Version

Interactive Discussion



Climatology of water and energy cycles in the Sahel

C. Velluet et al.

Title Page

Abstract

Introduction

Conclusions

References

Tables

Figures

◀

▶

◀

▶

Back

Close

Full Screen / Esc

Printer-friendly Version

Interactive Discussion

- Boulain, N., Cappelaere, B., Seguis, L., Favreau, G., and Gignoux, J.: Water balance and vegetation change in the Sahel: a case study at the watershed scale with an eco-hydrological model, *J. Arid Environ.*, 73, 1125–1135, doi:10.1016/j.jaridenv.2009.05.008, 2009b.
- Boulet, G., Kalma, J. D., Braud, I., and Vauclin, M.: An assessment of effective land surface parameterisation in regional-scale water balance studies, *J. Hydrol.*, 217, 225–238, doi:10.1016/s0022-1694(98)00246-7, 1999.
- Braud, I.: Spatial variability of surface properties and estimation of surface fluxes of a savannah, *Agr. Forest Meteorol.*, 89, 15–44, doi:10.1016/s0168-1923(97)00061-0, 1998.
- Braud, I.: SiSPAT, a Numerical Model of Water and Energy Fluxes in the Soil-Plant-Atmosphere Continuum – User’s Manual, L.T.H.E., Grenoble, France, 106 pp., 2000.
- Braud, I., Dantas-Antonino, A. C., Vauclin, M., Thony, J. L., and Ruelle, P.: A simple soil-plant-atmosphere transfer model (SiSPAT) development and field verification, *J. Hydrol.*, 166, 213–250, 1995.
- Braud, I., Bessemoulin, P., Monteny, B., Sicot, M., Vandervaere, J. P., and Vauclin, M.: Unidimensional modelling of a fallow savannah during the HAPEX-Sahel experiment using the SiSPAT model, *J. Hydrol.*, 188–189, 912–945, doi:10.1016/s0022-1694(96)03177-0, 1997.
- Brooks, R. H. and Corey, A. T.: Hydraulic Properties of Porous Media, *Hydrology Papers*, Colorado State University, 1964.
- Brunel, J. P., Walker, G. R., Dighton, J. C., and Monteny, B.: Use of stable isotopes of water to determine the origin of water used by the vegetation and to partition evapotranspiration. A case study from HAPEX-Sahel, *J. Hydrol.*, 188–189, 466–481, doi:10.1016/s0022-1694(96)03188-5, 1997.
- Burdine, N. T.: Relative permeability calculations from pore-size distribution data, *T. Am. I. Min. Met. Eng.*, 198, 71–78, 1953.
- Cappelaere, B., Descroix, L., Lebel, T., Boulain, N., Ramier, D., Laurent, J. P., Favreau, G., Boubkraoui, S., Boucher, M., Bouzou Moussa, I., Chaffard, V., Hiernaux, P., Is-soufou, H. B. A., Le Breton, E., Mamadou, I., Nazoumou, Y., Oi, M., Otlle, C., and Quantin, G.: The AMMA-CATCH experiment in the cultivated Sahelian area of south-west Niger – investigating water cycle response to a fluctuating climate and changing environment, *J. Hydrol.*, 375, 34–51, doi:10.1016/j.jhydrol.2009.06.021, 2009.
- Demarty, J., Otlle, C., François, C., Braud, I., and Frangi, J.-P.: Effect of aerodynamic resistance modelling on SiSPAT-RS simulated surface fluxes, *Agronomie*, 22, 641–650, doi:10.1051/agro:2002052, 2002.

Climatology of water and energy cycles in the Sahel

C. Velluet et al.

Title Page

Abstract

Introduction

Conclusions

References

Tables

Figures

◀

▶

◀

▶

Back

Close

Full Screen / Esc

Printer-friendly Version

Interactive Discussion



Demarty, J., Ottlé, C., Braud, I., Olioso, A., Frangi, J. P., Bastidas, L. A., and Gupta, H. V.: Using a multiobjective approach to retrieve information on surface properties used in a SVAT model, *J. Hydrol.*, 287, 214–236, doi:10.1016/j.jhydrol.2003.10.003, 2004.

Demarty, J., Ottlé, C., Braud, I., Olioso, A., Frangi, J. P., Gupta, H. V., and Bastidas, L. A.: Constraining a physically based Soil–Vegetation–Atmosphere Transfer model with surface water content and thermal infrared brightness temperature measurements using a multiobjective approach, *Water Resour. Res.*, 41, W01011, doi:10.1029/2004wr003695, 2005.

Descroix, L., Mahe, G., Lebel, T., Favreau, G., Galle, S., Gautier, E., Olivry, J. C., Albergel, J., Amogu, O., Cappelaere, B., Dessouassi, R., Diedhiou, A., Le Breton, E., Mamadou, I., and Sighomnou, D.: Spatio-temporal variability of hydrological regimes around the boundaries between Sahelian and Sudanian areas of West Africa: a synthesis, *J. Hydrol.*, 375, 90–102, doi:10.1016/j.jhydrol.2008.12.012, 2009.

Descroix, L., Laurent, J. P., Vauclin, M., Amogu, O., Boubkraoui, S., Ibrahim, B., Galle, S., Cappelaere, B., Bousquet, S., Mamadou, I., Le Breton, E., Lebel, T., Quantin, G., Ramier, D., and Boulain, N.: Experimental evidence of deep infiltration under sandy flats and gullies in the Sahel, *J. Hydrol.*, 424–425, 1–15, doi:10.1016/j.jhydrol.2011.11.019, 2012.

Estèves, M. and Lapetite, J. M.: A multi-scale approach of runoff generation in a Sahelian gully catchment: a case study in Niger, *CATENA*, 50, 255–271, doi:10.1016/s0341-8162(02)00136-4, 2003.

Ezzahar, J., Chehbouni, A., Hoedjes, J., Ramier, D., Boulain, N., Boubkraoui, S., Cappelaere, B., Descroix, L., Mougnot, B., and Timouk, F.: Combining scintillometer measurements and an aggregation scheme to estimate area-averaged latent heat flux during the AMMA experiment, *J. Hydrol.*, 375, 217–226, doi:10.1016/j.jhydrol.2009.01.010, 2009.

Favreau, G., Cappelaere, B., Massuel, S., Leblanc, M., Boucher, M., Boulain, N., and Leduc, C.: Land clearing, climate variability, and water resources increase in semiarid southwest Niger: a review, *Water Resour. Res.*, 45, W00A16, doi:10.1029/2007wr006785, 2009.

Federer, C. A.: A soil-plant-atmosphere model for transpiration and availability of soil water, *Water Resour. Res.*, 15, 555–562, doi:10.1029/WR015i003p00555, 1979.

Foken, T.: *Micrometeorology*, Springer-Verlag, Berlin, 306 pp., 2008.

Foken, T., Wimmer, F., Mauder, M., Thomas, C., and Liebenthal, C.: Some aspects of the energy balance closure problem, *Atmos. Chem. Phys.*, 6, 4395–4402, doi:10.5194/acp-6-4395-2006, 2006.

Climatology of water and energy cycles in the Sahel

C. Velluet et al.

Title Page

Abstract

Introduction

Conclusions

References

Tables

Figures

◀

▶

◀

▶

Back

Close

Full Screen / Esc

Printer-friendly Version

Interactive Discussion



François, C.: The potential of directional radiometric temperatures for monitoring soil and leaf temperature and soil moisture status, *Remote Sens. Environ.*, 80, 122–133, doi:10.1016/s0034-4257(01)00293-0, 2002.

Gash, J. H. C., Kabat, P., Monteny, B. A., Amadou, M., Bessemoulin, P., Billing, H., Blyth, E. M., deBruin, H. A. R., Elbers, J. A., Friborg, T., Harrison, G., Holwill, C. J., Lloyd, C. R., Lhomme, J. P., Moncrieff, J. B., Puech, D., Soegaard, H., Taupin, J. D., Tuzet, A., and Verhoef, A.: The variability of evaporation during the HAPEX-Sahel intensive observation period, *J. Hydrol.*, 188–189, 385–399, doi:10.1016/s0022-1694(96)03167-8, 1997.

Gaze, S. R., Simmonds, L. P., Brouwer, J., and Bouma, J.: Measurement of surface redistribution of rainfall and modelling its effect on water balance calculations for a millet field on sandy soil in Niger, *J. Hydrol.*, 188–189, 267–284, 1997.

Hanan, N. P. and Prince, S. D.: Stomatal conductance of West-Central supersite vegetation in HAPEX-Sahel: measurements and empirical models, *J. Hydrol.*, 188–189, 536–562, doi:10.1016/s0022-1694(96)03192-7, 1997.

Hoogmoed, W. B. and Klaij, M. C.: Soil management for crop production in the West African Sahel. I. Soil and climate parameters, *Soil Till. Res.*, 16, 85–103, doi:10.1016/0167-1987(90)90023-7, 1990.

Ibrahim, M., Favreau, G., Scanlon, B., Seidel, J.-L., Le Coz, M., Demarty, J., and Cappelaere, B.: Long-term increase in diffuse groundwater recharge following cultivation in the Sahel, West Africa, *Hydrogeol. J.*, accepted, 2014.

Issoufou, H. B.-A., Delzon, S., Laurent, J.-P., Saâdou, M., Mahamane, A., Cappelaere, B., Demarty, J., Rambal, S., and Seghieri, J.: Change in water loss regulation after canopy clearcut of a dominant shrub in Sahelian agrosystems, *Guiera senegalensis* J.F. Gmel, *Trees-Struct. Funct.*, 27, 1011–1022, doi:10.1007/s00468-013-0852-6, 2013.

Jackson, R. D.: Surface temperature and the surface energy balance, in: *Flow and Transport in the Natural Environment: Advances and Applications*, edited by: Steffen, W. L. and Denmead, O. J., Springer, Berlin/New York, 133–182, 1988.

Jacquemin, B. and Noilhan, J.: Sensitivity study and validation of a land surface parameterization using the HAPEX-MOBILHY data set, *Bound.-Lay. Meteorol.*, 52, 93–134, doi:10.1007/bf00123180, 1990.

Jarvis, P. G.: The interpretation of the variations in leaf water potential and stomatal conductance found in canopies in the field, *Philos. T. Roy. Soc. B*, 273, 593–610, doi:10.1098/rstb.1976.0035, 1976.

Climatology of water and energy cycles in the Sahel

C. Velluet et al.

Title Page

Abstract

Introduction

Conclusions

References

Tables

Figures

◀

▶

◀

▶

Back

Close

Full Screen / Esc

Printer-friendly Version

Interactive Discussion



Klajj, M. C. and Vachaud, G.: Seasonal water balance of a sandy soil in Niger cropped with pearl millet, based on profile moisture measurements, *Agr. Water Manage.*, 21, 313–330, doi:10.1016/0378-3774(92)90053-y, 1992.

Koster, R. D., Dirmeyer, P. A., Guo, Z., Bonan, G., Chan, E., Cox, P., Gordon, C. T., Kanae, S., Kowalczyk, E., Lawrence, D., Liu, P., Lu, C. H., Malyshev, S., McAvaney, B., Mitchell, K., Mocko, D., Oki, T., Oleson, K., Pitman, A., Sud, Y. C., Taylor, C. M., Verseghy, D., Vasic, R., Xue, Y., and Yamada, T.: Regions of strong coupling between soil moisture and precipitation, *Science*, 305, 1138–1140, doi:10.1126/science.1100217, 2004.

Lebel, T. and Ali, A.: Recent trends in the Central and Western Sahel rainfall regime (1990–2007), *J. Hydrol.*, 375, 52–64, doi:10.1016/j.jhydrol.2008.11.030, 2009.

Lebel, T., Cappelaere, B., Galle, S., Hanan, N., Kergoat, L., Levis, S., Vieux, B., Descroix, L., Gosset, M., Mougin, E., Peugeot, C., and Seguis, L.: AMMA-CATCH studies in the Sahelian region of West-Africa: an overview, *J. Hydrol.*, 375, 3–13, doi:10.1016/j.jhydrol.2009.03.020, 2009.

Leblanc, M. J., Favreau, G., Massuel, S., Tweed, S. O., Loireau, M., and Cappelaere, B.: Land clearance and hydrological change in the Sahel: SW Niger, *Global Planet. Change*, 61, 135–150, doi:10.1016/j.gloplacha.2007.08.011, 2008.

Lloyd, C. R., Bessemoulin, P., Cropley, F. D., Culf, A. D., Dolman, A. J., Elbers, J., Heusinkveld, B., Moncrieff, J. B., Monteny, B., and Verhoef, A.: A comparison of surface fluxes at the HAPEX-Sahel fallow bush sites, *J. Hydrol.*, 189, 400–425, 1997.

Lohou, F., Kergoat, L., Guichard, F., Boone, A., Cappelaere, B., Cohard, J.-M., Demarty, J., Galle, S., Grippa, M., Peugeot, C., Ramier, D., Taylor, C. M., and Timouk, F.: Surface response to rain events throughout the West African monsoon, *Atmos. Chem. Phys.*, 14, 3883–3898, doi:10.5194/acp-14-3883-2014, 2014.

Manyame, C., Morgan, C. L., Heilman, J. L., Fatondji, D., Gerard, B., and Payne, W. A.: Modeling hydraulic properties of sandy soils of Niger using pedotransfer functions, *Geoderma*, 141, 407–415, doi:10.1016/j.geoderma.2007.07.006, 2007.

Marshall, M., Tu, K., Funk, C., Michaelsen, J., Williams, P., Williams, C., Ardö, J., Boucher, M., Cappelaere, B., de Grandcourt, A., Nickless, A., Nouvellon, Y., Scholes, R., and Kutsch, W.: Improving operational land surface model canopy evapotranspiration in Africa using a direct remote sensing approach, *Hydrol. Earth Syst. Sci.*, 17, 1079–1091, doi:10.5194/hess-17-1079-2013, 2013.

Climatology of water and energy cycles in the Sahel

C. Velluet et al.

Title Page

Abstract

Introduction

Conclusions

References

Tables

Figures

◀

▶

◀

▶

Back

Close

Full Screen / Esc

Printer-friendly Version

Interactive Discussion

- Massuel, S., Favreau, G., Desclotres, M., Le Troquer, Y., Albouy, Y., and Cappelaere, B.: Deep infiltration through a sandy alluvial fan in semiarid Niger inferred from electrical conductivity survey, vadose zone chemistry and hydrological modelling, *CATENA*, 67, 105–118, doi:10.1016/j.catena.2006.02.009, 2006.
- 5 Massuel, S., Cappelaere, B., Favreau, G., Leduc, C., Lebel, T., and Vischel, T.: Integrated surface-groundwater modelling in the context of increasing water reserves of a Sahelian aquifer, *Hydrolog. Sci. J.*, 56, 1242–1264, doi:10.1080/02626667.2011.609171, 2011.
- Mauder, M. and Foken, T.: Documentation and Instruction Manual of the Eddy Covariance Software Package TK2, U. Bayreuth – Abt Mikrometeorologie, Bayreuth, Germany, 2004.
- 10 Merbold, L., Ardö, J., Arneith, A., Scholes, R. J., Nouvellon, Y., de Grandcourt, A., Archibald, S., Bonnefond, J. M., Boulain, N., Brueggemann, N., Bruemmer, C., Cappelaere, B., Ceschia, E., El-Khidir, H. A. M., El-Tahir, B. A., Falk, U., Lloyd, J., Kergoat, L., Le Dantec, V., Mougín, E., Muchinda, M., Mukelabai, M. M., Ramier, D., Roupsard, O., Timouk, F., Veenendaal, E. M., and Kutsch, W. L.: Precipitation as driver of carbon fluxes in 11 African ecosystems, *Biogeosciences*, 6, 1027–1041, doi:10.5194/bg-6-1027-2009, 2009.
- 15 Miller, R. L., Slingo, A., Barnard, J. C., and Kassianov, E.: Seasonal contrast in the surface energy balance of the Sahel, *J. Geophys. Res.*, 114, D00E05, doi:10.1029/2008jd010521, 2009.
- Milly, P. C. D.: Moisture and heat transport in hysteretic, inhomogeneous porous media: a matrix head-based formulation and a numerical model, *Water Resour. Res.*, 18, 489–498, doi:10.1029/WR018i003p00489, 1982.
- 20 Monteny, B. A.: HAPEX-Sahel 1992, Campagne de Mesures Supersite Central Est, ORSTOM, Montpellier, France, 230 pp., 1993.
- Pellarin, T., Laurent, J. P., Cappelaere, B., Decharme, B., Descroix, L., and Ramier, D.: Hydrological modelling and associated microwave emission of a semi-arid region in South-western Niger, *J. Hydrol.*, 375, 262–272, doi:10.1016/j.jhydrol.2008.12.003, 2009.
- 25 Peugeot, C., Esteves, M., Galle, S., Rajot, J.-L., and Vandervaere, J. P.: Runoff generation processes: results and analysis of field data collected at the East Central Super-site of the HAPEX-Sahel experiment, *J. Hydrol.*, 188–189, 179–202, doi:10.1016/s0022-1694(96)03159-9, 1997.
- 30 Ramier, D., Boulain, N., Cappelaere, B., Timouk, F., Rabanit, M., Lloyd, C. R., Boubkraoui, S., Metayer, F., Descroix, L., and Wawrzyniak, V.: Towards an understanding of coupled physical

Climatology of water and energy cycles in the Sahel

C. Velluet et al.

Title Page

Abstract

Introduction

Conclusions

References

Tables

Figures

◀

▶

◀

▶

Back

Close

Full Screen / Esc

Printer-friendly Version

Interactive Discussion



and biological processes in the cultivated Sahel – 1. Energy and water, *J. Hydrol.*, 375, 204–216, doi:10.1016/j.jhydrol.2008.12.002, 2009.

Ridler, M. E., Sandholt, I., Butts, M., Lerer, S., Mougin, E., Timouk, F., Kergoat, L., and Madsen, H.: Calibrating a soil–vegetation–atmosphere transfer model with remote sensing estimates of surface temperature and soil surface moisture in a semi arid environment, *J. Hydrol.*, 436–437, 1–12, doi:10.1016/j.jhydrol.2012.01.047, 2012.

Rockström, J. and Valentin, C.: Hillslope dynamics of on-farm generation of surface water flows: the case of rain-fed cultivation of pearl millet on sandy soil in the Sahel, *Agr. Water Manage.*, 33, 183–210, doi:10.1016/s0378-3774(96)01282-6, 1997.

Rockström, J., Jansson, P. E., and Barron, J.: Seasonal rainfall partitioning under runoff and runoff conditions on sandy soil in Niger. On-farm measurements and water balance modelling, *J. Hydrol.*, 210, 68–92, doi:10.1016/s0022-1694(98)00176-0, 1998.

Rothfuss, Y., Braud, I., Le Moine, N., Biron, P., Durand, J.-L., Vauclin, M., and Bariac, T.: Factors controlling the isotopic partitioning between soil evaporation and plant transpiration: assessment using a multi-objective calibration of SiSPAT-Isotope under controlled conditions, *J. Hydrol.*, 442–443, 75–88, doi:10.1016/j.jhydrol.2012.03.041, 2012.

Saux-Picart, S., Otle, C., Decharme, B., Andre, C., Zribi, M., Perrier, A., Coudert, B., Boulain, N., Cappelaere, B., Descroix, L., and Ramier, D.: Water and energy budgets simulation over the AMMA-Niger super-site spatially constrained with remote sensing data, *J. Hydrol.*, 375, 287–295, doi:10.1016/j.jhydrol.2008.12.023, 2009a.

Saux-Picart, S., Otle, C., Perrier, A., Decharme, B., Coudert, B., Zribi, M., Boulain, N., Cappelaere, B., and Ramier, D.: SEtHyS_Savannah: a multiple source land surface model applied to Sahelian landscapes, *Agr. Forest Meteorol.*, 149, 1421–1432, doi:10.1016/j.agrformet.2009.03.013, 2009b.

Schlenker, W. and Lobell, D. B.: Robust negative impacts of climate change on African agriculture, *Environ. Res. Lett.*, 5, 014010, doi:10.1088/1748-9326/5/1/014010, 2010.

Shin, Y., Mohanty, B. P., and Ines, A. V. M.: Soil hydraulic properties in one-dimensional layered soil profile using layer-specific soil moisture assimilation scheme, *Water Resour. Res.*, 48, W06529, doi:10.1029/2010wr009581, 2012.

Shuttleworth, W. J. and Wallace, J. S.: Evaporation from sparse crops – an energy combination theory, *Q. J. Roy. Meteor. Soc.*, 111, 839–855, doi:10.1256/smsqj.46909, 1985.

Šimůnek, J., Angulo-Jaramillo, R., Schaap, M. G., Vandervaere, J.-P., and van Genuchten, M. T.: Using an inverse method to estimate the hydraulic properties of

Climatology of water and energy cycles in the Sahel

C. Velluet et al.

[Title Page](#)

[Abstract](#)

[Introduction](#)

[Conclusions](#)

[References](#)

[Tables](#)

[Figures](#)

[⏪](#)

[⏩](#)

[◀](#)

[▶](#)

[Back](#)

[Close](#)

[Full Screen / Esc](#)

[Printer-friendly Version](#)

[Interactive Discussion](#)

- crusted soils from tension-disc infiltrometer data, *Geoderma*, 86, 61–81, doi:10.1016/s0016-7061(98)00035-4, 1998.
- Sjöström, M., Ardö, J., Arneth, A., Boulain, N., Cappelaere, B., Eklundh, L., de Grandcourt, A., Kutsch, W. L., Merbold, L., Nouvellon, Y., Scholes, R. J., Schubert, P., Seaquist, J., and Veenendaal, E. M.: Exploring the potential of MODIS EVI for modeling gross primary production across African ecosystems, *Remote Sens. Environ.*, 115, 1081–1089, doi:10.1016/j.rse.2010.12.013, 2011.
- Sjöström, M., Zhao, M., Archibald, S., Arneth, A., Cappelaere, B., Falk, U., de Grandcourt, A., Hanan, N., Kergoat, L., Kutsch, W. L., Merbold, L., Mougou, E., Nickless, A., Nouvellon, Y., Scholes, R. J., Veenendaal, E. M., and Ardö, J.: Evaluation of MODIS gross primary productivity for Africa using eddy covariance data, *Remote Sens. Environ.*, 131, 275–286, 2013.
- Soegaard, H. and Boegh, E.: Estimation of evapotranspiration from a millet crop in the Sahel combining sap flow, leaf-area index and eddy-correlation technique, *J. Hydrol.*, 166, 265–282, doi:10.1016/0022-1694(94)05094-e, 1995.
- Taconet, O., Bernard, R., and Vidal-Madjar, D.: Evapotranspiration over an agricultural region using a surface flux/temperature model based on NOAA-AVHRR data, *J. Clim. Appl. Meteorol.*, 25, 284–307, 1986.
- Tanguy, M., Baille, A., González-Real, M. M., Lloyd, C., Cappelaere, B., Kergoat, L., and Cohard, J. M.: A new parameterisation scheme of ground heat flux for land surface flux retrieval from remote sensing information, *J. Hydrol.*, 454–455, 113–122, doi:10.1016/j.jhydrol.2012.06.002, 2012.
- Taylor, C. M., Gounou, A., Guichard, F., Harris, P. P., Ellis, R. J., Couvreur, F., and De Kauwe, M.: Frequency of Sahelian storm initiation enhanced over mesoscale soil-moisture patterns, *Nat. Geosci.*, 4, 430–433, doi:10.1038/ngeo1173, 2011.
- Taylor, C. M., de Jeu, R. A. M., Guichard, F., Harris, P. P., and Dorigo, W. A.: Afternoon rain more likely over drier soils, *Nature*, 489, 423–426, doi:10.1038/nature11377, 2012.
- Timouk, F., Kergoat, L., Mougou, E., Lloyd, C. R., Ceschia, E., Cohard, J. M., de Rosnay, P., Hiernaux, P., Demarez, V., and Taylor, C. M.: Response of surface energy balance to water regime and vegetation development in a Sahelian landscape, *J. Hydrol.*, 375, 178–189, doi:10.1016/j.jhydrol.2009.04.022, 2009.
- Trenberth, K. E., Fasullo, J. T., and Kiehl, J.: Earth's global energy budget, *B. Am. Meteorol. Soc.*, 90, 311–323, doi:10.1175/2008BAMS2634.1, 2009.

Climatology of water and energy cycles in the Sahel

C. Velluet et al.

[Title Page](#)

[Abstract](#)

[Introduction](#)

[Conclusions](#)

[References](#)

[Tables](#)

[Figures](#)

[⏪](#)

[⏩](#)

[◀](#)

[▶](#)

[Back](#)

[Close](#)

[Full Screen / Esc](#)

[Printer-friendly Version](#)

[Interactive Discussion](#)



- Tuzet, A., Castell, J. F., Perrier, A., and Zurfluh, O.: Flux heterogeneity and evapotranspiration partitioning in a sparse canopy: the fallow savanna, *J. Hydrol.*, 188–189, 482–493, doi:10.1016/s0022-1694(96)03189-7, 1997.
- Vandervaere, J. P., Peugeot, C., Vauclin, M., Angulo Jaramillo, R., and Lebel, T.: Estimating hydraulic conductivity of crusted soils using disc infiltrometers and minitensiometers, *J. Hydrol.*, 188–189, 203–223, doi:10.1016/s0022-1694(96)03160-5, 1997.
- van Genuchten, M. T.: A closed-form equation for predicting the hydraulic conductivity of unsaturated soils, *Soil Sci. Soc. Am. J.*, 44, 892–898, doi:10.2136/sssaj1980.03615995004400050002x, 1980.
- van Vliet, N., Reenberg, A., and Rasmussen, L. V.: Scientific documentation of crop land changes in the Sahel: a half empty box of knowledge to support policy?, *J. Arid Environ.*, 95, 1–13, doi:10.1016/j.jaridenv.2013.03.010, 2013.
- Velluet, C.: Multi-year modelling and analysis of the hydrologic and energetic functioning of two dominant ecosystems in the cultivated Sahel (SW Niger), Ph.D., E.D. Sibaghe, University Montpellier 2, Montpellier, France, 2014 (in French).
- Verhoef, A., Allen, S. J., and Lloyd, C. R.: Seasonal variation of surface energy balance over two Sahelian surfaces, *Int. J. Climatol.*, 19, 1267–1277, doi:10.1002/(sici)1097-0088(199909)19:11<1267::aid-joc418>3.0.co;2-s, 1999.
- Verhoef, A., Otlé, C., Cappelaere, B., Murray, T., Saux Picart, S., Zribi, A., Maignan, F., Boulain, N., Demarty, J., and Ramier, D.: Spatio-temporal surface soil heat flux estimates from satellite data; results for the AMMA experiment, Fakara supersite, *Agr. Forest Meteorol.*, 154–155, 55–66, doi:10.1016/j.agrformet.2011.08.003, 2012.
- Wallace, J. S., Wright, I. R., Stewart, J. B., and Holwill, C. J.: The Sahelian energy balance experiment (SEBEX): ground based measurements and their potential for spatial extrapolation using satellite data, *Adv. Space Res.*, 11, 131–141, 1991.
- Weiss, M., Baret, F., Smith, G. J., and Jonckheere, I.: Methods for in situ leaf area index measurement, part II: from gap fraction to leaf area index: retrieval methods and sampling strategies, *Agr. Forest Meteorol.*, 121, 17–53, 2004.
- Wolters, D., van Heerwaarden, C. C., de Arellano, J. V. G., Cappelaere, B., and Ramier, D.: Effects of soil moisture gradients on the path and the intensity of a West African squall line, *Q. J. Roy. Meteor. Soc.*, 136, 2162–2175, doi:10.1002/qj.712, 2010.

Climatology of water and energy cycles in the Sahel

C. Velluet et al.

Title Page

Abstract

Introduction

Conclusions

References

Tables

Figures

◀

▶

◀

▶

Back

Close

Full Screen / Esc

Printer-friendly Version

Interactive Discussion



Table 1. Description of permanent GAI-recording stations in the Wankama fallow and millet plots.

Instrument	Measurements	Height or depth	Frequency
Above ground			
Campbell CSAT-3 sonic anemometer (Campbell Scientific, Inc, Logan, USA)	3-D wind speed and direction Sonic air temperature	5 m	20 Hz
LI-COR LI-7500 infrared gas analyzer (LI-COR Biosciences, Lincoln, USA)	CO ₂ and H ₂ O concentrations Air pressure	5 m	20 Hz
Kipp & Zonen CNR1 radiometer (Kipp & Zonen, Delft, the Netherlands)	Shortwave (0.3–2.8 μm) and longwave (5–50 μm) incoming and outgoing radiation	3.5 m (fallow) 2.5 m (millet)	1 min
Wind monitor RM103 (Young, USA)	2-D wind speed and direction	3 m	1 min
Vaisala HMP45C (Vaisala Oyj, Helsinki, Finland)	Air temperature and relative humidity	3 m	1 min
Soil measurements			
Campbell CS616 water content reflectometer (×6)	Soil volumetric water content	–0.1, –0.5, –1.0, –1.5, –2.0, –2.5 m	1 min
Campbell T108 temperature probe (×6)	Soil temperature	–0.1, –0.5, –1.0, –1.5, –2.0, –2.5 m	1 min
Hukseflux HFP01SC heat flux plates (×3, averaged) (Hukseflux, Delft, the Netherlands)	Surface soil heat flux	–0.05 m	1 min

Table 2. Vegetation, surface and soil parameters in SiSPAT model (Braud, 2000), with values either calibrated (parameter groups C and D; see Sect. 2.4 for group definitions) or non-calibrated (parameter groups A and B). Right column shows prior values or ranges obtained from literature (^a Braud, 2000; ^b Jacquemin and Noihlan, 1990; ^c Hanan and Prince, 1997; ^d Monteny, 1993; ^e Jackson, 1988, and Demarty et al., 2004; ^f Roujean, J. L., personal communication in Braud, 1997; ^g François, 2002; ^h Braud et al., 1997; ⁱ Šimůnek et al., 1998; ^j Vandervaere et al., 1997; ^k Manyame et al., 2007; ^l Klaij and Vachaud, 1992; ^m Rockström and Valentin, 1997; ⁿ Hoogmoed and Klaij, 1990; ^o Gaze et al., 1997).

Parameter	Unit	Group	Fallow field	Millet field	Literature values	
					Fallow	Millet
Vegetation parameters						
Vapor deficit factor in plant stress function	Pa ⁻¹	B	2.50 × 10 ⁻⁴	2.50 × 10 ⁻⁴	2.50 × 10 ^{-4a}	
Critical leaf water potential	m	B	-140	-140	-140 ^h	-
Maximum stomatal resistance	sm ⁻¹	B	5000	5000	5000 ^b	
Minimum stomatal resistance	sm ⁻¹	C	70	100	80 ^c	125 ^c
Total plant resistance	sm ⁻¹ _{root}	C	1.50 × 10 ¹³	6.50 × 10 ¹²	6.50 × 10 ^{12h}	
Root density profile			<i>(Time invariant)</i>	<i>(At peak development)</i>	adjusted from	
+ P1: maximum root density @ depth	m _{root} m _{soil} ⁻³ @ m	C	22 900 @ 0.03 to 0.1	25 000 @ 0.03 to 0.1	Braud et al. (1997)	Rockström et al. (1998)
+ P2: intermediate root density @ depth	m _{root} m _{soil} ⁻³ @ m	C	1603 @ 0.85	5000 @ 0.50		
+ P3: maximal root depth	m	C	3.5	2.3		

Radiative surface parameters						
Bare soil albedo $\alpha = f(\theta)$:						
+ dry albedo ($\theta = 0.04$)	-	A	0.345	0.340	-	-
+ wet albedo ($\theta = 0.18$)	-	A	0.190	0.200	-	-
Bare soil emissivity	-	B	0.97	0.97	0.97 ^d	
Vegetation emissivity	-	B	0.98	0.98	0.98 ^e	
Vegetation albedo	-	C	0.20	0.22	0.20 ^f	-
Interception parameter:						
+ infrared	-	B	0.825	0.825	For a spherical canopy: 0.825 ^g	
+ short waves	-	C	0.45	0.55	0.50 ^g	

Title Page

Abstract

Introduction

Conclusions

References

Tables

Figures

⏪

⏩

⏴

⏵

Back

Close

Full Screen / Esc

Printer-friendly Version

Interactive Discussion



Climatology of water and energy cycles in the Sahel

C. Velluet et al.

Table 2. Continued.

Parameter	Unit	Group	Fallow field					Millet field					Literature values		
			H1 0–0.01	H2 0.01–0.2	H3 0.2–0.7	H4 0.7–1.2	H5 1.2–4.0	H1 0–0.01	H2 0.01–0.2	H3 0.2–0.7	H4 0.7–1.2	H5 1.2–4.0	Crust	Soil	
Soil parameters	Horizon depth (m)														
Dry bulk density	kg m ⁻³	A	1.70	1.70	1.80	1.70	1.75	1.70	1.70	1.80	1.70	1.75			
Porosity Φ	–	A	0.358	0.358	0.321	0.358	0.340	0.358	0.358	0.321	0.358	0.340			
Sand	%	A	85	85	85	85	85	85	85	85	85	85			
Clay+Silt	%	A	13	13	13	13	13	13	13	13	13	13			
Organic matter	%	A	2	2	2	2	2	2	2	2	2	2			
Dry volumetric heat capacity	10 ⁶ J m ⁻³ K ⁻¹	A	1.28	1.28	1.36	1.28	1.32	1.28	1.28	1.36	1.28	1.32		= 2.10 ⁶ (1 – Φ) ³	
Saturated water content θ_{sat}	m ³ m ⁻³	A	0.30	0.30	0.30	0.30	0.30	0.30	0.30	0.30	0.30	0.30	[0.25; 0.35] ^{h,i,j}	[0.25; 0.42] ^{h,i,j,k}	
Residual water content θ_r	m ³ m ⁻³	A	0.01	0.012	0.028	0.027	0.037	0.01	0.023	0.046	0.047	0.056	[0; 0.03] ^{h,i}	[0; 0.06] ^{h,i,k,l}	
Retention curve shape parameter h_g	m	D	–0.85	–0.60	–0.40	–0.30	–0.20	–0.50	–0.30	–0.30	–0.20	–0.20	[–24; –0.31] ^{h,i}	[–0.60; –0.06] ^{h,i,k}	
Retention curve shape parameter n	–	D	2.75	3.00	3.10	3.00	3.30	2.75	3.00	3.00	3.00	3.00	[2.35; 3.53] ^{h,i}	[2.55; 4.19] ^{h,i,k}	
Saturated hydraulic conductivity K_{sat}	ms ⁻¹	D	1 × 10 ⁻⁷	7 × 10 ⁻⁵	5 × 10 ⁻⁵	7 × 10 ⁻⁵	7 × 10 ⁻⁵	2.5 × 10 ⁻⁷	5 × 10 ⁻⁵	[1.7 × 10 ⁻⁸ ; 2 × 10 ⁻⁶] ^{h,i,j}	[4 × 10 ⁻⁶ ; 7 × 10 ⁻⁵] ^{h-o}				
Conductivity curve form parameter β	–	D	6.0	5.0	5.0	4.5	5.0	6.0	5.0	5.5	5.5	6.0		[4.3; 6.1] ^h	
Soil thermal conductivity scaling parameter	–	D	2.00	1.50	1.00	1.00	1.00	1.00	0.75	0.85	1.00	1.00		Default value: 1.00	

Title Page

Abstract Introduction

Conclusions References

Tables Figures

◀ ▶

◀ ▶

Back Close

Full Screen / Esc

Printer-friendly Version

Interactive Discussion



Table 3. Model skill scores against observed half-hourly surface fluxes and soil moisture and temperature. Each cell shows first the score for the whole study period (May 2005–April 2012; plain characters), then the score for the calibration period only (May 2006–April 2008; italic characters). RMSE is root mean square error, NSE Nash–Sutcliffe efficiency, r correlation coefficient (units for RMSE and bias are given with variable type, NSE and r are dimensionless); see Eq. (1) for other abbreviations.

	Fallow field								Millet field							
	RMSE		bias		NSE		r		RMSE		bias		NSE		r	
Surface fluxes (Wm^{-2})																
SWout	9.0	<i>9.8</i>	-0.5	<i>2.4</i>	0.99	<i>0.99</i>	>0.99	<i>>0.99</i>	9.9	<i>11.5</i>	-4.3	<i>-4.5</i>	0.99	<i>0.99</i>	>0.99	<i>>0.99</i>
LWout	15.6	<i>18.3</i>	-3.0	<i>-6.7</i>	0.95	<i>0.93</i>	0.99	<i>0.99</i>	15.9	<i>14.9</i>	7.2	<i>6.5</i>	0.94	<i>0.95</i>	0.98	<i>0.98</i>
Rn	14.5	<i>13.3</i>	4.7	<i>5.5</i>	0.99	<i>>0.99</i>	>0.99	<i>>0.99</i>	18.5	<i>18.9</i>	-1.9	<i>-1.1</i>	0.99	<i>0.99</i>	>0.99	<i>>0.99</i>
$G_{-0.05m}$	17.7	<i>15.0</i>	-4.3	<i>-4.1</i>	0.93	<i>0.95</i>	0.97	<i>0.98</i>	18.1	<i>14.2</i>	-3.8	<i>-3.3</i>	0.92	<i>0.95</i>	0.96	<i>0.97</i>
H	26.8	<i>27.8</i>	-5.2	<i>-7.7</i>	0.90	<i>0.91</i>	0.96	<i>0.96</i>	29.0	<i>26.0</i>	-0.8	<i>-1.7</i>	0.87	<i>0.89</i>	0.94	<i>0.95</i>
LE	33.3	<i>38.7</i>	-3.3	<i>-2.2</i>	0.77	<i>0.76</i>	0.88	<i>0.88</i>	26.2	<i>27.4</i>	-2.0	<i>-0.3</i>	0.78	<i>0.77</i>	0.89	<i>0.88</i>
Soil water storage (mm)																
Whole column to 2.5 m depth	9.3	<i>13.7</i>	-1.8	<i>1.8</i>	0.68	<i>0.55</i>	0.92	<i>0.95</i>	15.3	<i>15.8</i>	0.6	<i>3.8</i>	0.83	<i>0.87</i>	0.93	<i>0.96</i>
H1–H2 (0–0.2 m)	1.6	<i>1.5</i>	0.1	<i>0.2</i>	0.87	<i>0.92</i>	0.96	<i>0.98</i>	1.1	<i>1.2</i>	-0.3	<i>-0.3</i>	0.94	<i>0.94</i>	0.97	<i>0.97</i>
H3 (0.2–0.7 m)	3.6	<i>3.7</i>	-1.3	<i>-0.9</i>	0.74	<i>0.82</i>	0.90	<i>0.94</i>	5.2	<i>4.9</i>	1.1	<i>1.3</i>	0.72	<i>0.78</i>	0.96	<i>0.98</i>
H4 (0.7–1.2 m)	5.4	<i>8.0</i>	1.7	<i>2.6</i>	<0	<i><0</i>	0.80	<i>0.85</i>	4.3	<i>3.6</i>	-0.1	<i>0.1</i>	0.76	<i>0.87</i>	0.92	<i>0.97</i>
H5 (1.2–2.5 m)	3.8	<i>4.4</i>	-2.4	<i>-0.2</i>	<0	<i><0</i>	0.71	<i>0.93</i>	10.1	<i>11.2</i>	0.0	<i>2.7</i>	0.75	<i>0.78</i>	0.88	<i>0.91</i>
Point soil temperatures ($^{\circ}C$)																
0.1 m	2.5	<i>2.8</i>	-1.9	<i>-2.6</i>	0.80	<i>0.77</i>	0.96	<i>0.98</i>	1.9	<i>1.3</i>	-0.6	<i>-0.4</i>	0.90	<i>0.96</i>	0.96	<i>0.98</i>
0.5 m	1.7	<i>2.2</i>	-1.5	<i>-2.1</i>	0.73	<i>0.65</i>	0.97	<i>0.98</i>	1.0	<i>0.8</i>	-0.5	<i>-0.4</i>	0.90	<i>0.95</i>	0.96	<i>0.98</i>
1.0 m	1.4	<i>1.8</i>	-1.3	<i>-1.7</i>	0.70	<i>0.62</i>	0.97	<i>0.98</i>	0.9	<i>0.7</i>	-0.6	<i>-0.4</i>	0.87	<i>0.94</i>	0.96	<i>0.98</i>
1.5 m	1.3	<i>1.6</i>	-1.2	<i>-1.5</i>	0.62	<i>0.54</i>	0.97	<i>0.98</i>	0.8	<i>0.6</i>	-0.5	<i>-0.4</i>	0.84	<i>0.92</i>	0.95	<i>0.98</i>
2.0 m	1.1	<i>1.3</i>	-1.0	<i>-1.2</i>	0.56	<i>0.48</i>	0.95	<i>0.96</i>	0.8	<i>0.6</i>	-0.4	<i>-0.3</i>	0.79	<i>0.89</i>	0.94	<i>0.97</i>
2.5 m	0.9	<i>1.0</i>	-0.7	<i>-0.9</i>	0.59	<i>0.53</i>	0.93	<i>0.94</i>	0.8	<i>0.7</i>	-0.4	<i>-0.2</i>	0.72	<i>0.82</i>	0.92	<i>0.95</i>

Title Page

Abstract Introduction

Conclusions References

Tables Figures

◀ ▶

◀ ▶

Back Close

Full Screen / Esc

Printer-friendly Version

Interactive Discussion



Climatology of water and energy cycles in the Sahel

C. Velluet et al.

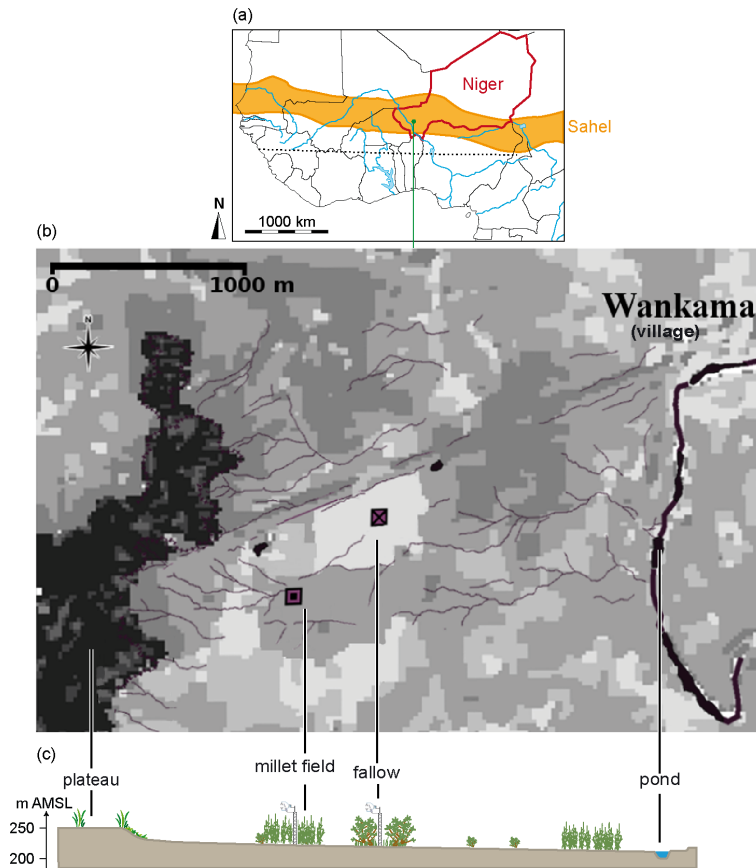


Fig. 1. Situation of study plots: **(a)** location in Sahelian southwestern Niger, West Africa, **(b)** planar and **(c)** cross-sectional views of Wankama hillslope with plot locations (modified after Boulain et al., 2009a; vegetation and towers not sketched to scale).

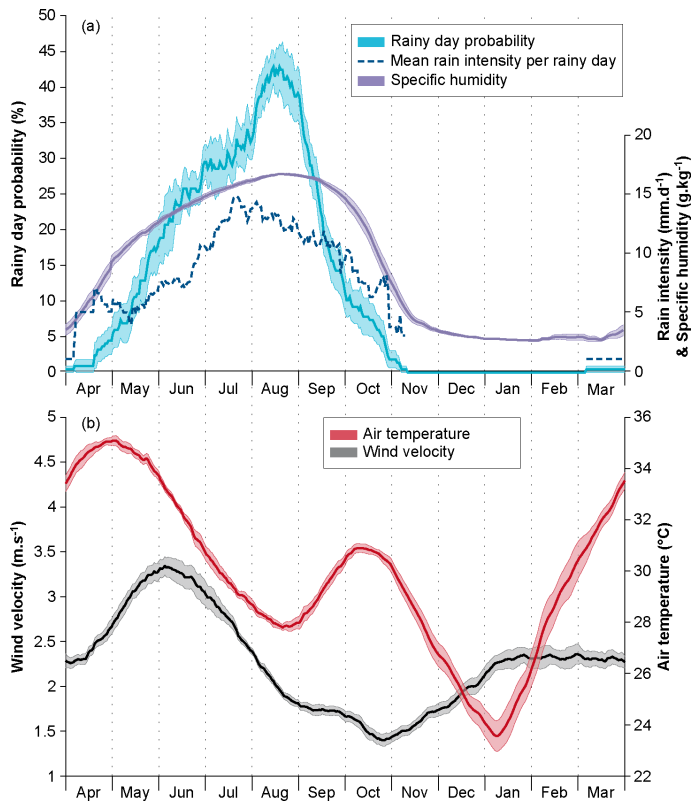


Fig. 2. Mean seasonal courses of meteorological variables in Wankama catchment: **(a)** probability and mean rain intensity of rainy day, specific humidity; **(b)** air temperature and 3 m-wind velocity. Values are 30 d running averages for 2005–2012, from instruments described in Table 1. Light-colored areas represent a variation of \pm one standard estimation error.

Climatology of water and energy cycles in the Sahel

C. Velluet et al.

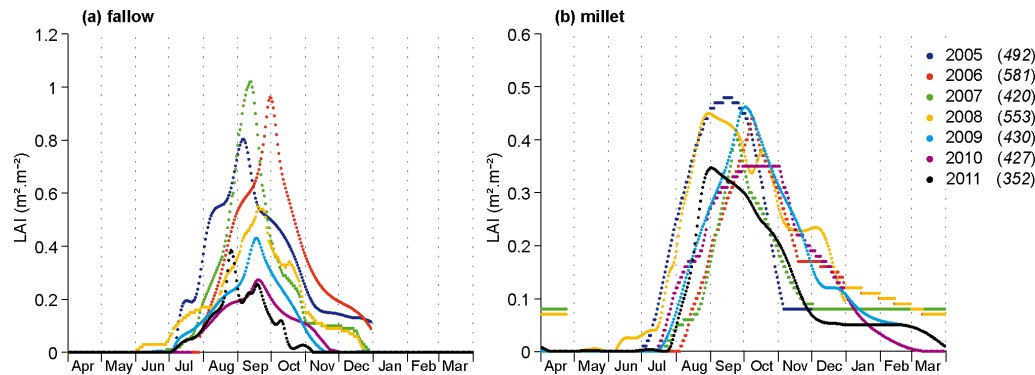


Fig. 3. Seasonal course of daily LAI at fallow **(a)** and millet **(b)** plots, for each growing season of 2005–2011 (in brackets: total rainfall, in mm).

Title Page

Abstract

Introduction

Conclusions

References

Tables

Figures

◀

▶

◀

▶

Back

Close

Full Screen / Esc

Printer-friendly Version

Interactive Discussion



Climatology of water and energy cycles in the Sahel

C. Velluet et al.

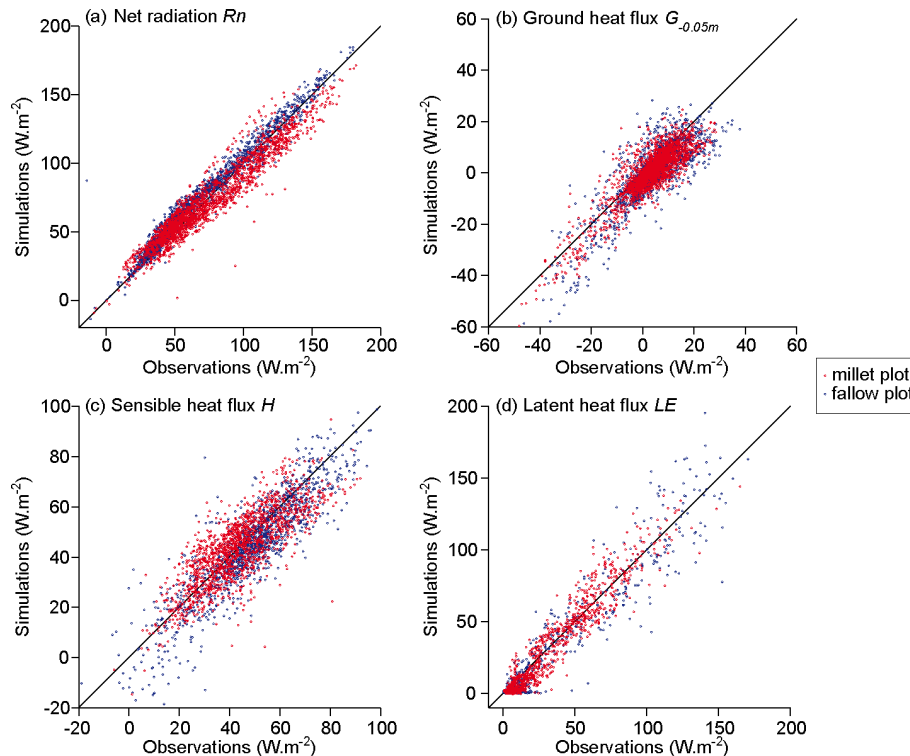


Fig. 4. Simulated vs. field-estimated daily energy fluxes of **(a)** net radiation, **(b)** ground heat (at 5 cm-depth), **(c)** sensible heat, and **(d)** latent heat, for the fallow (blue) and millet (red) plots, through the 2005–2012 study period (only days with no missing data are represented).

Climatology of water and energy cycles in the Sahel

C. Velluet et al.

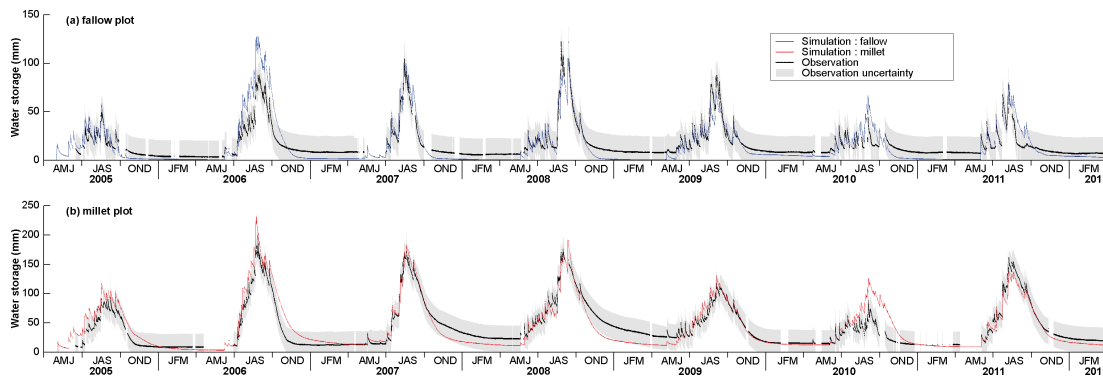


Fig. 5. Observed and simulated courses of total water storage in 0–2.5 m soil layer at fallow **(a)** and millet **(b)** plots over 2005–2012 (storage taken above residual water content θ_r).

Title Page

Abstract

Introduction

Conclusions

References

Tables

Figures

◀

▶

◀

▶

Back

Close

Full Screen / Esc

Printer-friendly Version

Interactive Discussion



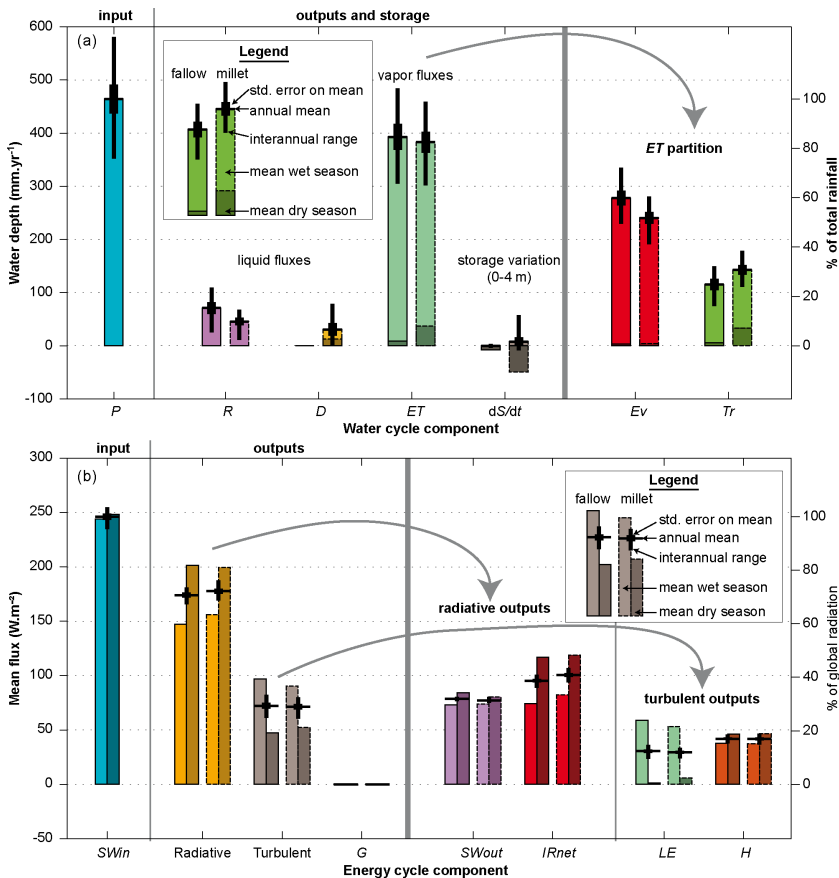


Fig. 7. Estimated water **(a)** and energy **(b)** budgets at annual and semi-annual scales: interannual ranges (black thin bars), annual means with standard estimation errors (black thick bars), and seasons means (light color for wet season, May–October; dark color for dry season, November–April), for the fallow (solid contours) and millet (dashed contours) plots. See Eq. (1) for abbreviations.

Climatology of water and energy cycles in the Sahel

C. Velluet et al.

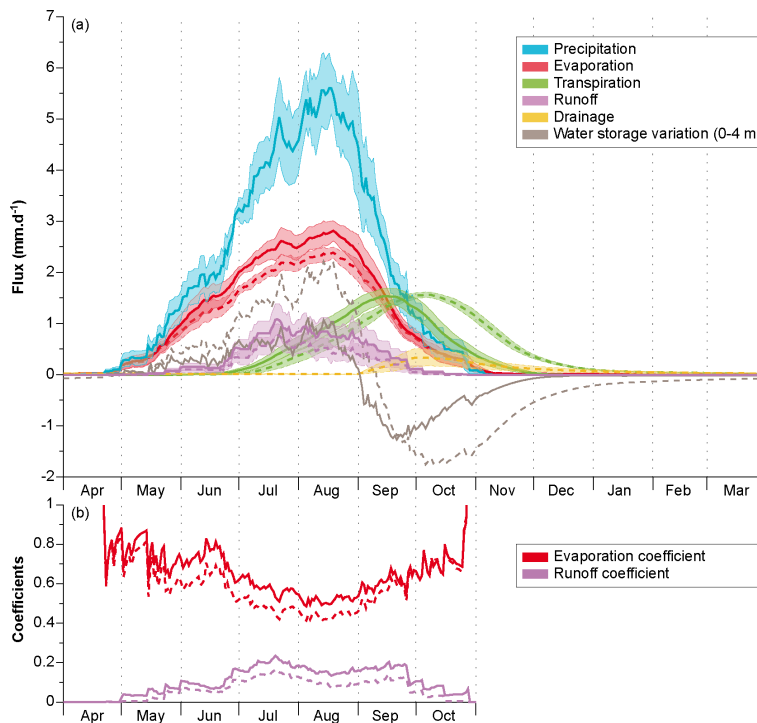


Fig. 8. Estimated mean seasonal courses of water cycle components, for fallow (solid lines) and millet (dashed lines) plots: **(a)** fluxes, and rate of storage change in 0–4 m soil column; **(b)** ratios of above evaporation and runoff means to rainfall. Means are computed across years and over a 30 d running window. Light-colored areas represent a variation of \pm one standard estimation error around the estimated mean (not shown for storage change in **(a)**, for legibility).

[Title Page](#)
[Abstract](#)
[Introduction](#)
[Conclusions](#)
[References](#)
[Tables](#)
[Figures](#)
[⏪](#)
[⏩](#)
[◀](#)
[▶](#)
[Back](#)
[Close](#)
[Full Screen / Esc](#)
[Printer-friendly Version](#)
[Interactive Discussion](#)

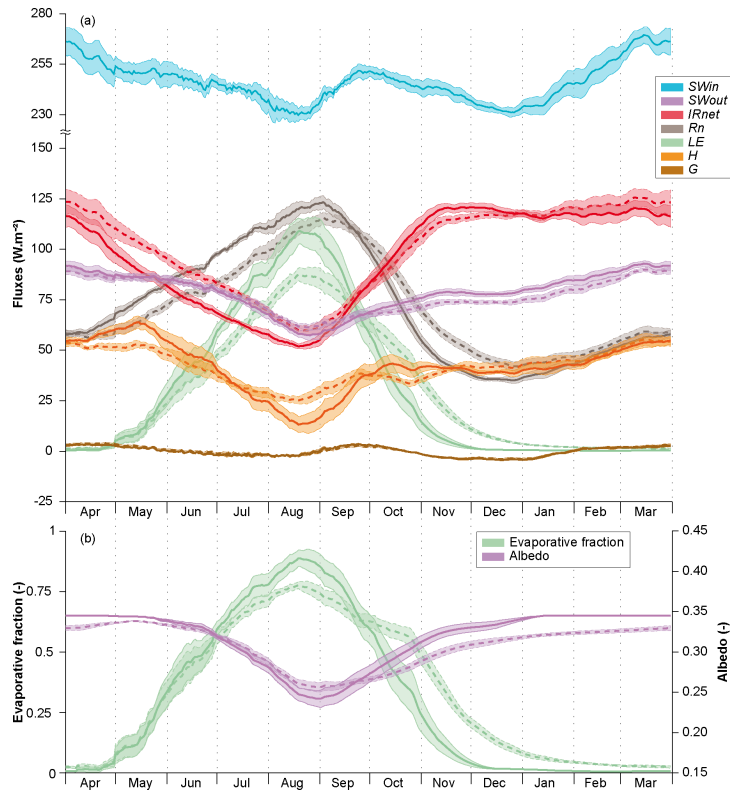



Fig. 9. Estimated mean seasonal courses of energy cycle components, for fallow (solid lines) and millet (dashed lines) plots: **(a)** incoming shortwave and outgoing fluxes; **(b)** evaporative fraction and albedo. See Eq. (1) for abbreviations, and Fig. 8 for further explanation of curves and colored areas.

Climatology of water and energy cycles in the Sahel

C. Velluet et al.

Title Page

Abstract

Introduction

Conclusions

References

Tables

Figures

◀

▶

◀

▶

Back

Close

Full Screen / Esc

Printer-friendly Version

Interactive Discussion



Climatology of water and energy cycles in the Sahel

C. Velluet et al.

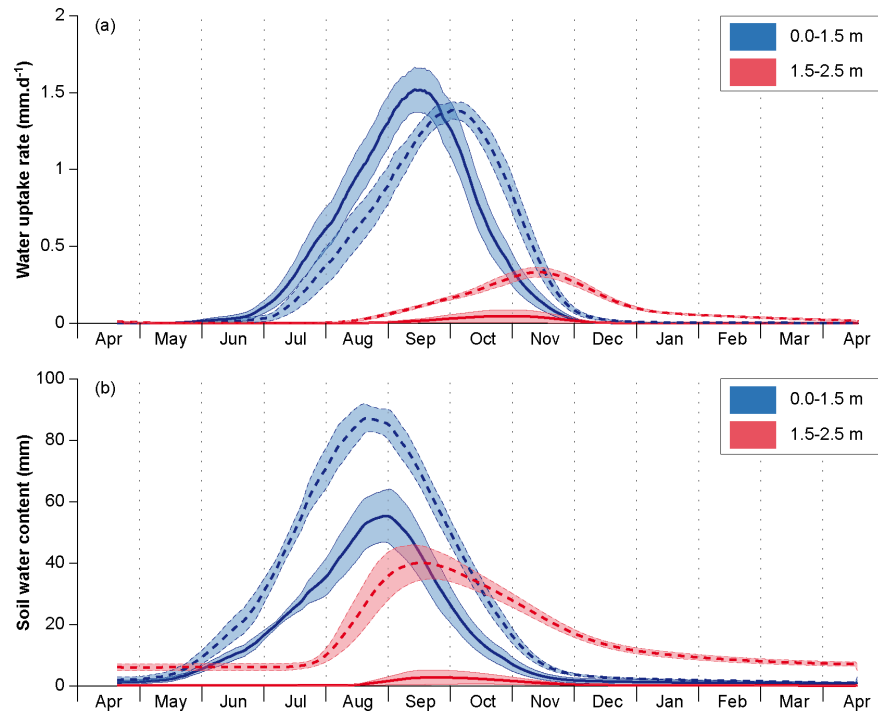


Fig. 10. Estimated mean seasonal courses of **(a)** water uptake by plant roots and **(b)** soil water storage (above θ_r), separately in two active root zone layers (depths in legend), for fallow (solid lines) and millet (dashed lines) plots. See Fig. 8 for further explanation of curves and colored areas.